SPARK COUNTER NEUTRON DETECTOR FOR HIGH-TEMPERATURE APPLICATIONS

Final Report

Submitted by

Geoffrey G. Eichholz
Professor of Nuclear Engineering
Georgia Institute of Technology
Atlanta, Georgia 30332

to the

Division of Reactor Development and Technology
U. S. Atomic Energy Commission

Contract No. AT-(40-1)-3563

Project A-966

June, 1969

GTA

Pub
deposit
11-9-71

TABLE OF CONTENTS

	Page
List of Illustrations	v
Abstract	vii
Introduction	1
Counter Design	5
Detector Characteristics	15
Converter Material	21
Filling Gases	26
Operating Range	30
High Temperature Operation	39
Conclusions	47
Project Personnel	49
References	51

List of Illustrations

Figure		Page
1.	2" Detector -- Diagram of Construction.	6
2.	Photograph of 2" Detector	7
3.	1" Detector -- Diagram of Construction.	9
4.	1" Detector -- Disassembled View.	10
5.	1" Detector -- Assembled View	11
6.	Stainless Steel Detector -- Assembled View.	12
7.	Stainless Steel Detector -- Disassembled View	13
8.	Shielding Plug for Vertical Beam Hole	16
9.	Counter Assembly for Insertion into Vertical Beam Hole	17
10.	Typical Counter Characteristic.	18
11.	Quench Circuit.	20
12.	Boron Nitride Heating Curves.	23
13.	Effect of Gap Width on Operating Characteristics. . . .	25
14.	Variation in Gap Number -- Effect on Operating Characteristics	27
15.	Effect of Flow Rate on Counter Characteristics.	28
16.	Operating Characteristics for Stainless Steel Detector, Ar-N_2 Filling	29
17.	Close-up View of Stainless Steel Detector with Needle Valve.	31
18.	Linearity Plot -- Relation of Count Rate to Neutron Flux.	32
19.	Variation of Supply Voltage at High Flux Levels	35
20.	Shift in Supply Voltage to Maintain Constant Counts.	36
21.	Muffle Furnace Set Up at Reactor Beam Hole.	40

List of Illustrations (Concluded)

Figure		Page
22.	View of Experimental Assembly at Beam Port.	41
23.	Temperature Characteristics of Spark Counters	42,43
24.	Variation in Optimum Supply Voltage with Temperature	44
25.	Resistance-Temperature Plot for Porcelain Insulator	45

Abstract

Spark counters of the "corrugated electrode" type have been designed and tested for use as neutron detectors in high neutron fluxes and at high temperatures. These detectors consist of a gas-filled coaxial assembly, in which circular ridges, acting as spark gap electrodes with the cylindrical outer container, are interleaved with boron-containing disks, which act as neutron converters by producing alpha particles by the $B^{10}(n,\alpha)Li^7$ reaction. These alpha particles trigger a spark across the gap, producing a large current pulse that is readily detected and counted.

With argon or helium gas fillings, such counters were operated at temperatures up to 1076°F at which point the leakage currents across the ceramic insulator seals became excessive.

The counters were tested in a wide range of neutron fluxes, up to 6×10^{10} n/cm^{2}sec, and gamma-ray fields, up to 2×10^5 R/hr. The counters were found to have a linear response in neutron fluxes up to 6×10^9 n/cm^2 sec in the presence of gamma-ray fields of the order of 10^4 R/hr. Above that level the response became increasingly nonlinear as gas ionization due to primary and secondary gamma-rays became significant and ultimately suppressed the spark mechanism at fluxes of the order of 3×10^{10} n/cm^2 sec. Attempts to extend the range of high flux response significantly by variations in gas pressure have not been successful. The detector sensitivity at low and medium fluxes is of the order of 10^{-8} counts/neutron and can be varied by increasing or decreasing the number of converter disks.

Introduction

Spark counters are finding increasing applications in present day nuclear physics, primarily as detectors of high-energy charged particles in the form of large-volume spark chambers. Such chambers lend themselves to on-line computer evaluation of results and a considerable technology is growing up around them. An entirely different direction of application of spark counters is that related to their use as simple, rugged monitors of radiation and of contamination. One example of such detectors is the multiwire corrugated-plate detector developed by the present author in 1952 (1) and applied to the detection of surface alpha contamination and the comparison of uranium ore samples. The present work is an outgrowth of this work aimed at the adaptation of such detectors to high level, charged particle detection and to neutron detection by means of boron-containing converters (2,3).

With the advent of high-power, high-temperature reactors, there is a need for low-efficiency, reliable neutron detectors that will operate at quite high temperatures for unlimited times in a high neutron flux and gamma radiation environment. At the present time the detector that approaches these requirements most closely is the coaxial cable detector (4), which has a limited life, however, and provides only very small signal amplitudes. Goodings (5) has described high temperature neutron detectors capable of operating up to 550°C, as in-pile D.C. ionization chambers or fission chambers with a pulse output transformer. Recently Todt (6) has described a vacuum charge-collection chamber for high-flux detection of transient neutron pulses. Hawkings (7) has reviewed thermocouple instruments for neutron monitoring.

In view of the small output signals and the relative complexity of construction and operation of some of the conventional detectors, it has seemed worthwhile to develop an alternative neutron detector for high-flux, high-temperature operation. Based on previous work on corrugated-plate spark counters (3), that type of detector appeared to offer a promising approach, and the present project was set up to develop such a detector, to be capable, if possible, of operating at temperatures up to 1600°F and neutron fluxes up to 10^{15} n/cm^{2}sec.

The principle of operation of the spark counter is simple. If two conducting points or ridges are placed opposite each other with a small air gap or inside a gas-filled enclosure, a corona field will be set up around the points whenever the conductors are maintained at an appropriate electric potential. Any ionizing particle passing through the gap region will then initiate a spark discharge. The magnitude and appearance of the spark depend on the electrode gap spacing, the applied voltage, the gas filling used, the gas pressure, and the time constant of the associated circuits.

Any heavily ionizing particle, such as a proton or an alpha particle, may trigger such a spark under appropriate conditions. In the absence of any ionizing event, no discharge will occur unless the applied voltage is raised to a level that the corona can extend across the gap and dielectric breakdown of the gas occurs. Below this breakdown voltage, few sparks would be initiated in the absence of a source of charged particles, provided the electrode surfaces are smooth and clean. As a result of the absence of spontaneous arcing under normal conditions, the background count of such an electrode system is very low. This low background count in the absence of heavily ionizing radiation, together with the large signal amplitude and the simple configuration possible, makes this type of detector attractive as a reliable, low-background detector of heavy charged particles.

Closely related to these detectors are the "spark chambers" that are currently popular as large volume detectors of high-energy nuclear particles (8-10). In that case, multiple arrays of wires and plates are used to provide a large three-dimensional sensitive volume, whose voltage can be pulsed by a counter telescope to minimize spurious events.

The spark counters under consideration in this report are much less sophisticated devices, with an intentionally low detection efficiency to provide for operation in high radiation fluxes with a near-continuous sensitivity. In order to adapt such a detector to neutron detection, a converter such as boron must be introduced into the space near the spark gap. Natural boron contains the isotope boron-10 with an abundance of 19.9%. Boron-10 has a cross section of 3587 barns for the reaction $B^{10}(n,\alpha)Li^{7}$ at thermal neutron energies. If a boron-containing surface is placed close to the spark gap, the alpha particles emerging from it whenever a neutron is captured by the boron atoms will trigger the spark gap. By counting the sparks initiated in this fashion, a measure of the neutron flux is obtained.

In the present application, the spark gaps are formed by a ridged metal spindle placed along the axis of a hollow metal cylinder, which provides the outer electrode of the gap system. The neutron converter in the form of boron nitride disks is placed close to and between neighboring spark gaps, ensuring a favorable geometry for triggering the sparks by emerging alpha particles. By choosing the number of spark gaps and converter disks, the efficiency of the detector can be adjusted over a range of values. Limitations on the usable number of gaps and converter disks are imposed by the need for obtaining an accurately uniform spacing between the electrodes for uniform breakdown characteristics and by the need for confining the detector volume to a region of essentially constant neutron flux.

From the nature of the objectives of this project, the counter development fell into three basic aspects: design of a suitable detector configuration and selection of appropriate circuit characteristics, measurement of detector characteristics under different conditions of gas filling and neutron flux levels, and high temperature characteristics of the detector. These will be dealt with in turn in the following sections.

Counter Design

The present counter evolved from the corrugated-plate spark counter concept (2,3) which was retained for early tests on comparative performance with different gases and different electrode spacings. Using an americium-241 alpha source and a transparent enclosure, it was possible to observe the nature and characteristics of the sparks in different gases and for various applied voltages. Some of that preliminary work has been described in the July 1967 Progress Report (11) and need not be repeated here in detail.

Since it was planned to develop a cylindrical detector, a prototype was designed early which consisted of a series of washers of two sizes arranged alternately with boron nitride converter disks on a spindle which could be mounted inside a cylindrical aluminum shell. This counter is illustrated diagrammatically in Fig. 1. Fig. 2 shows a photograph of this detector. One end plate could be removed and replaced by a concentric Lucite shell on which an americium-241 source was mounted. This arrangement made it possible to observe visually the spark phenomena under various operating conditions. Some difficulties arose from the need to maintain accurate coaxial alignment of the spindle and washer assembly in the Kovar feed-through connectors, but these were overcome with some experience.

Boron nitride was found to be a convenient, relatively inexpensive converter material. It is a stable, machineable material with good temperature characteristics. For the initial stages of the projects, disks were cut from 1-inch diameter boron nitride rod. For the later detectors, $\frac{3}{4}$" diameter, thin BN washers of standard design were obtained from Union

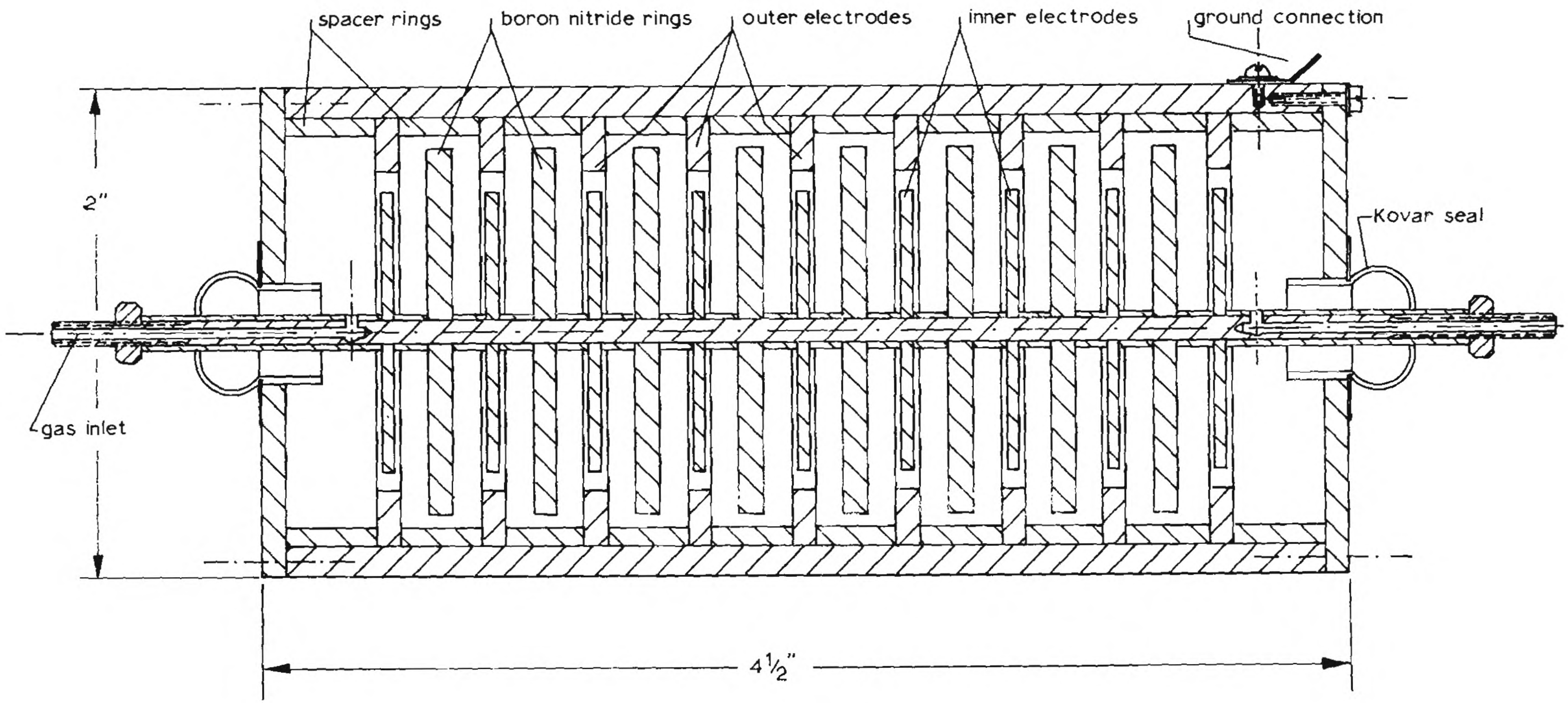

Fig. 1. 2" Detector -- Diagram of Construction

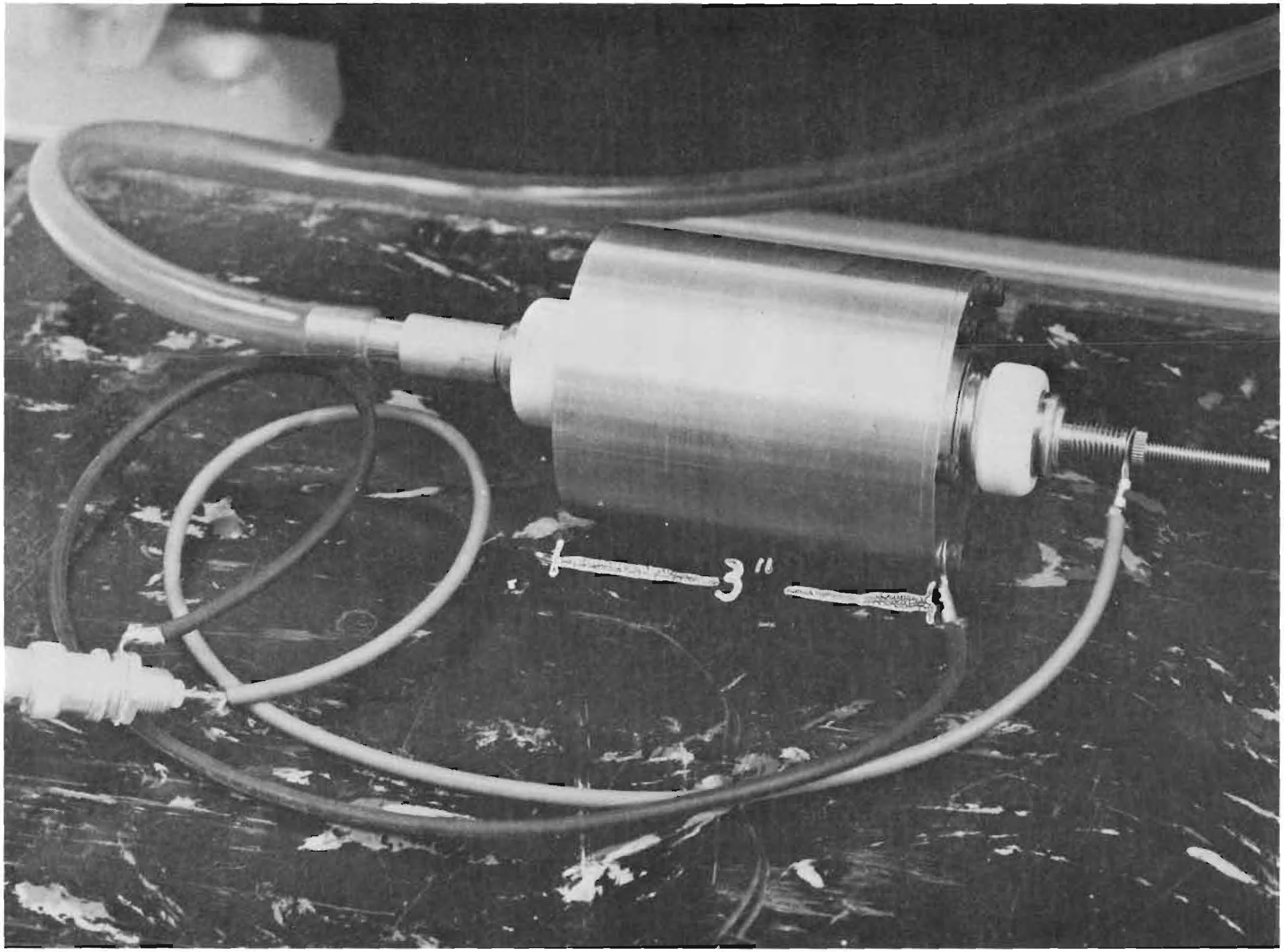

Fig. 2. Photograph of 2" Detector

Carbide Corporation, Carbon Products Division, and proved quite satisfactory, even when a narrow slot had to be cut radially into each of them.

In order to meet project specifications for a one-inch diameter detector, a simplified version of the previous detector was designed and constructed. Fig. 3 shows a diagram of this counter design. It consisted of an inner spindle arrangement with integral ridges incorporated in it, which formed the inner, positive electrodes of the spark gap. The aluminum outer barrel provided a smooth continuous outer negative electrode, and this configuration was found to be adequate and much more convenient to make and to assemble. Slotted boron nitride disks, as shown in Fig. 4, were fitted over the recessed portions of the spindle to act as converters. Alignment of inner and outer electrodes depended on the Teflon seals at each end. Figs. 4 and 5 show the disassembled and assembled counter. Electrical contact was made to the inner and outer electrodes through a solder lug fastened to a set screw on the outer barrel and another hooked on the threaded part of the spindle. The filling gas entered the counter through a hollow canal running in one end of the spindle.

Since aluminum with its relatively low melting point and high coefficient of thermal expansion did not appear to be suitable for high temperature operation, several stainless steel detectors were made along similar lines. One of these is illustrated in Figs. 6 and 7 in assembled and disassembled form. In these detectors, concentric porcelain feed-throughs were utilized as end seals and only three spark gaps with 2-4 converter disks were used, to keep the detection efficiency down. As can be seen from the figures, the counter dimensions are $2\frac{1}{2}''$ long by $1''$ diameter, not

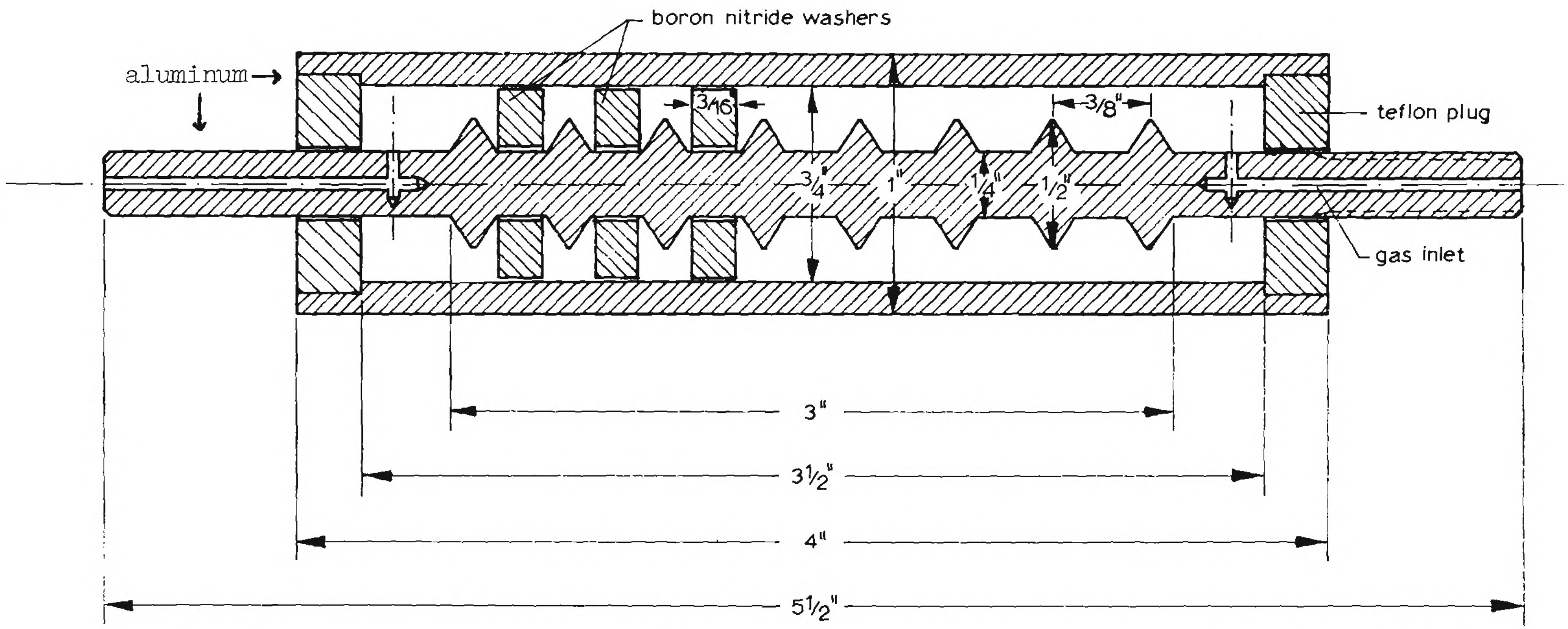

Fig. 3. 1" Detector -- Diagram of Construction

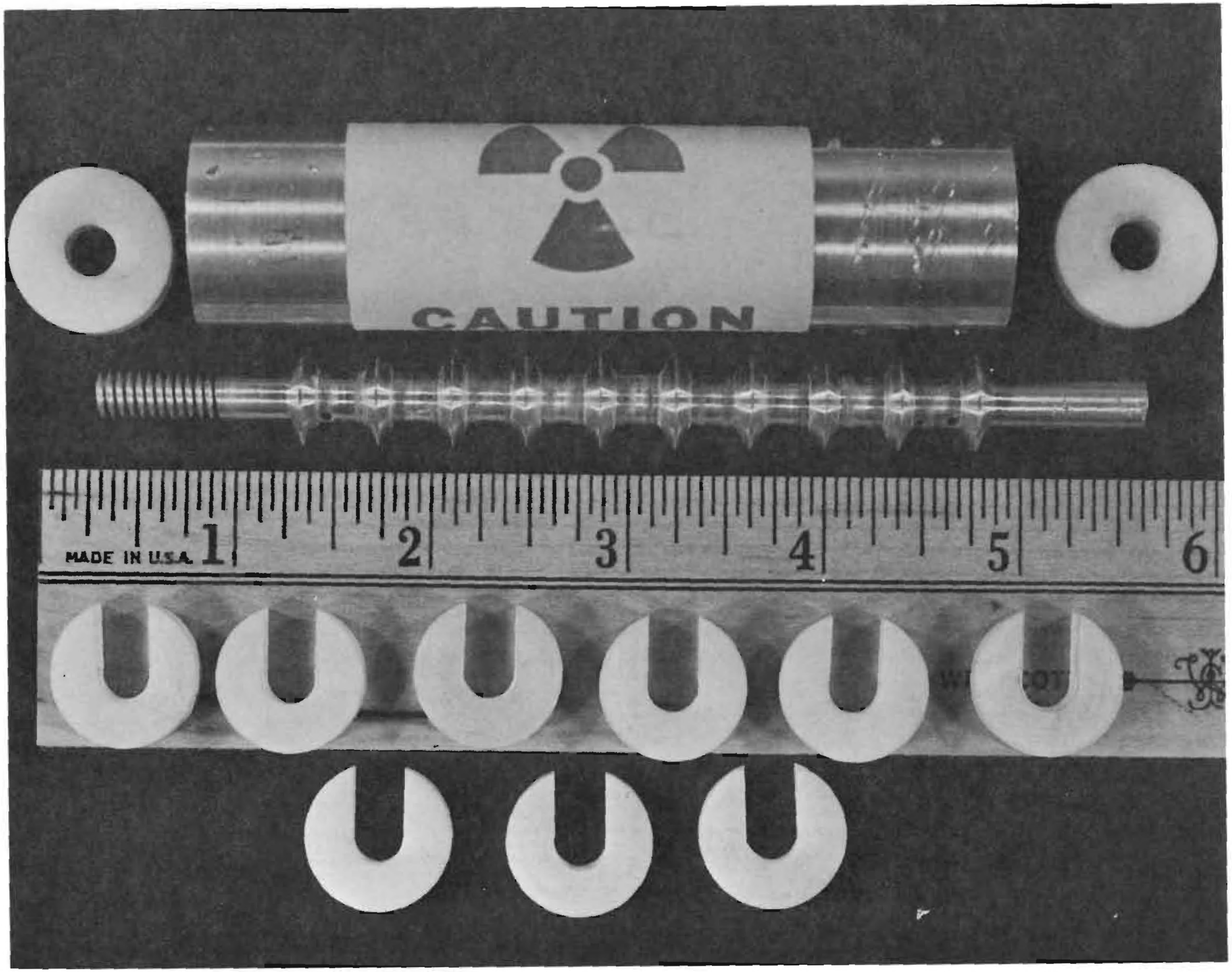

Fig. 4. 1" Detector -- Disassembled View

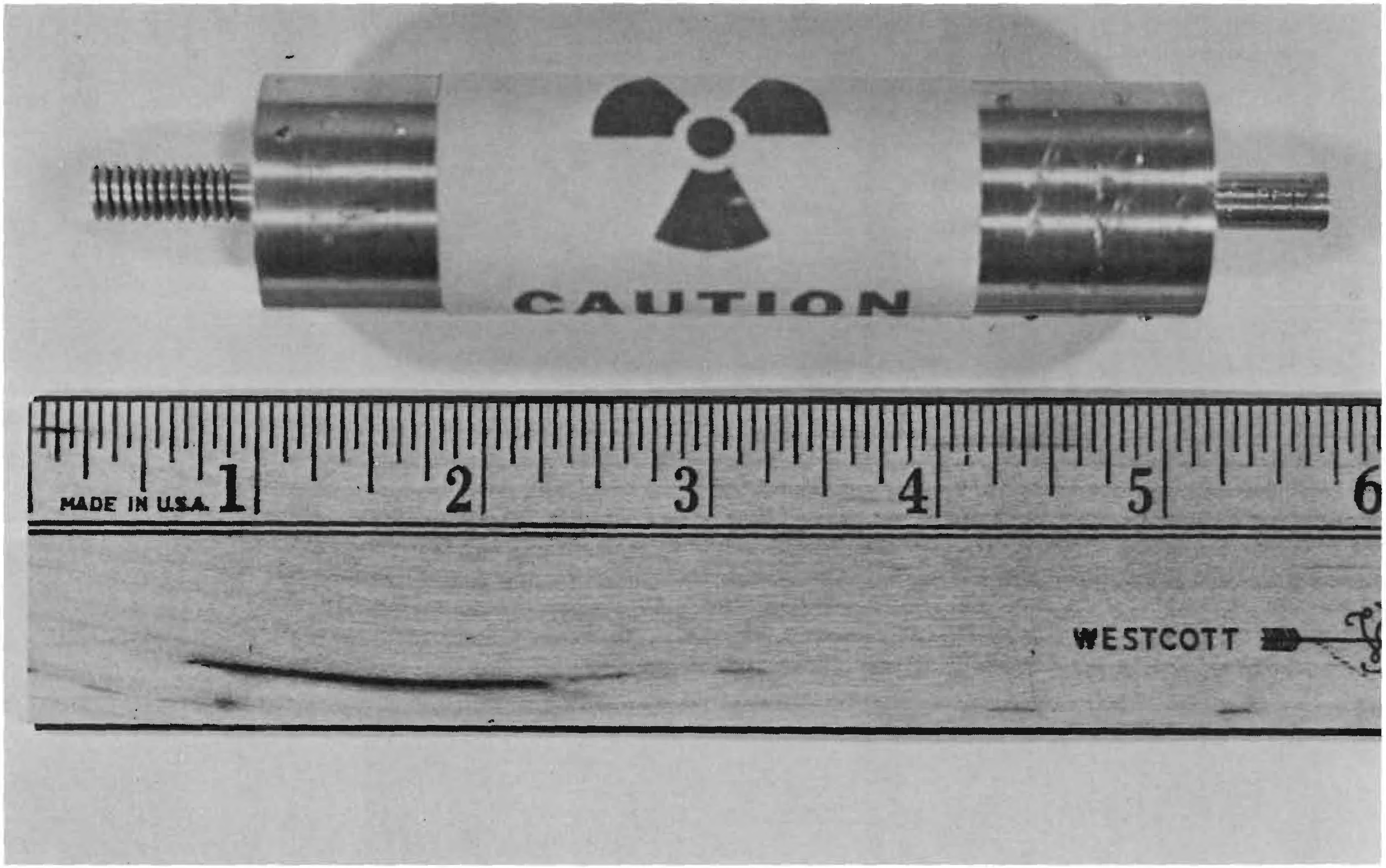

Fig. 5. 1" Detector -- Assembled View

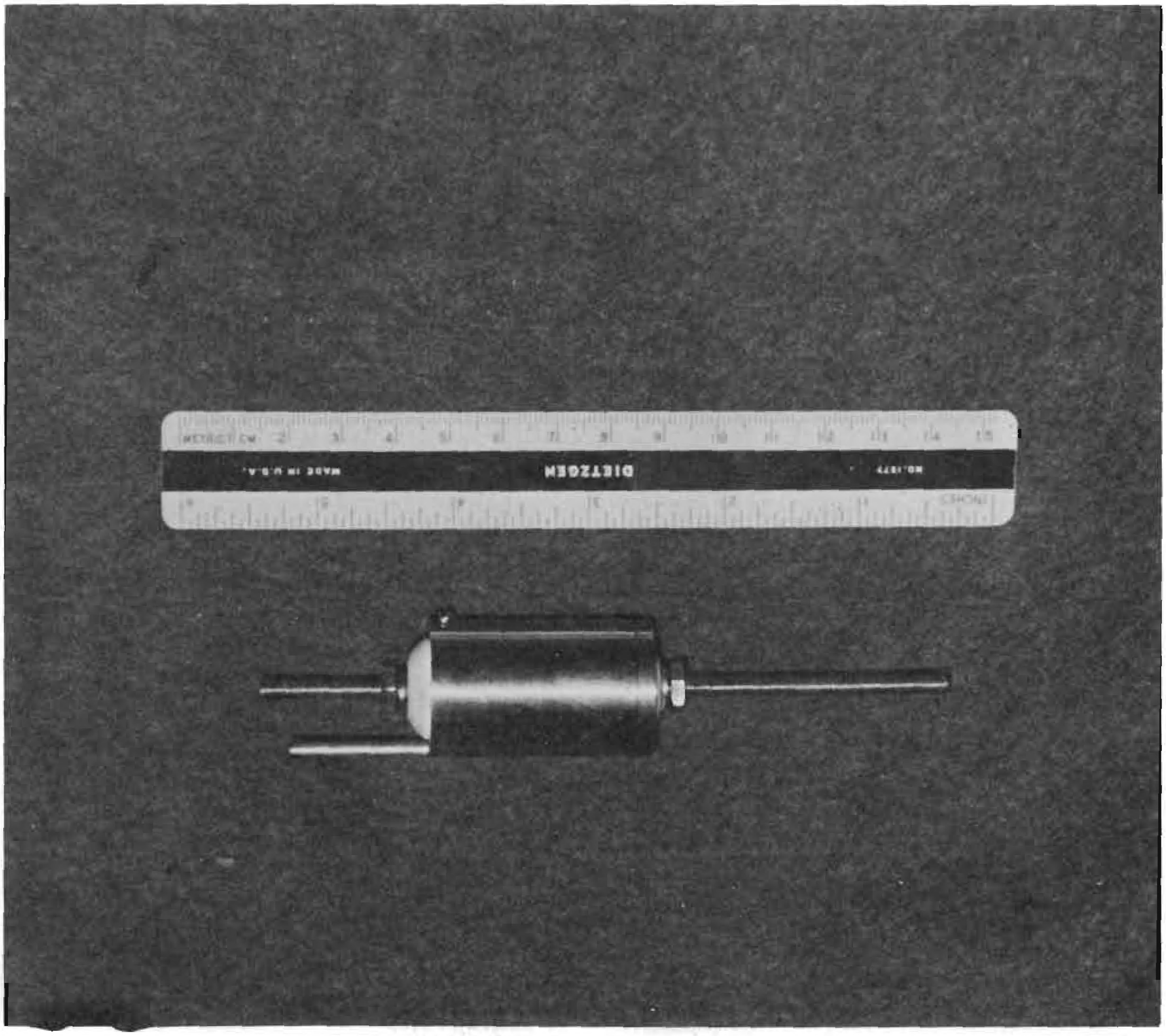

Fig. 6. Stainless Steel Detector -- Assembled View

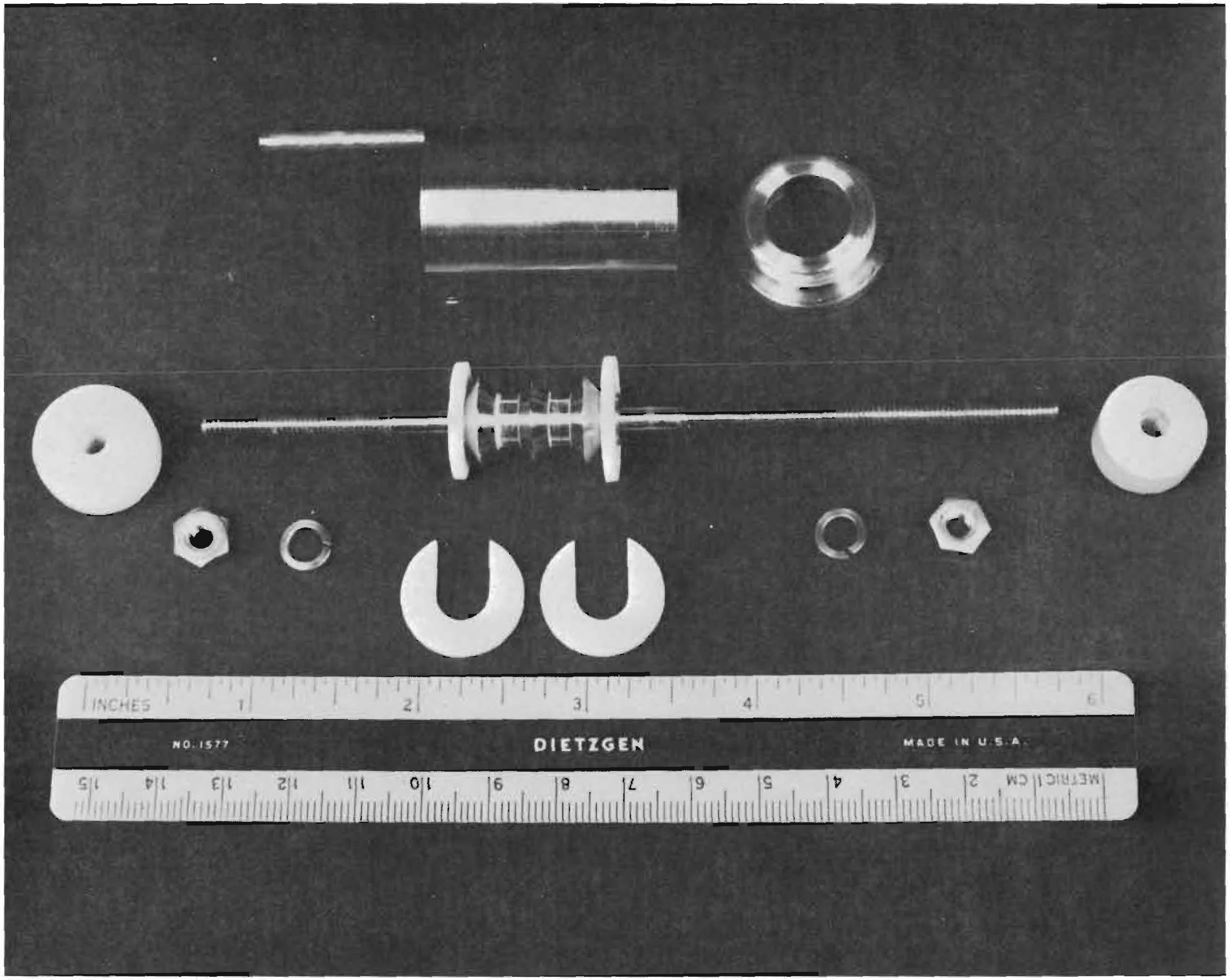

Fig. 7. Stainless Steel Detector -- Disassembled View

counting the threaded spindle which can be cut to any convenient length. This clearly constitutes a simple, compact, and rugged detector that should find many uses. In the particular detector shown, the gas filling was introduced through the thin filling tube entering the shell parallel to the spindle. Another detector, shown in a later section, was filled through a tube tapped into the middle of the outer barrel. Type 304 stainless steel was used for all these detectors.

Detector Characteristics

The various detectors were tested in thermal neutron radiation fields at several beam holes of the Georgia Tech Research Reactor, a one megawatt heavy-water cooled and moderated reactor with a peak neutron flux of the order of 10^{14} n/cm^{2}sec. Two positions at the face of the reactor were used; one at the end of a horizontal beam hole (H-2), whose inner end penetrates the core tank, providing neutron fluxes of the order of 10^8 n/cm^{2}sec at full power; the other at a collimated beam position inside the "medical facility," a heavily shielded room with a heavy protective door, where neutron fluxes up to 2×10^7 n/cm^{2}sec are available. A special beam catcher was made to back up any test at the H-2 beam hole.

For detector measurements in higher neutron fluxes, the detector system was inserted into a vertical beam hole adjacent to the core tank from a position at the top of the reactor. A special shield plug with three spiraled channels to carry leads was made up to fit into the outer biological shield. This plug is shown in Fig. 8. From this plug, a long aluminum framework was suspended, at the bottom of which the detector was mounted as well as a rhodium flux monitor. This whole assembly is shown in Fig. 9, suspended above the reactor prior to insertion into the beam hole.

The various detectors were tested with and without exposure to the neutron beam, and the operating characteristics were plotted in every case. Fig. 10 shows a typical characteristic plot; the useful operating region lies between the two curves. The best operating voltage, for optimum signal-to-background ratio, lies just above the threshold of operation, and it is seen that the background count remains effectively zero over a

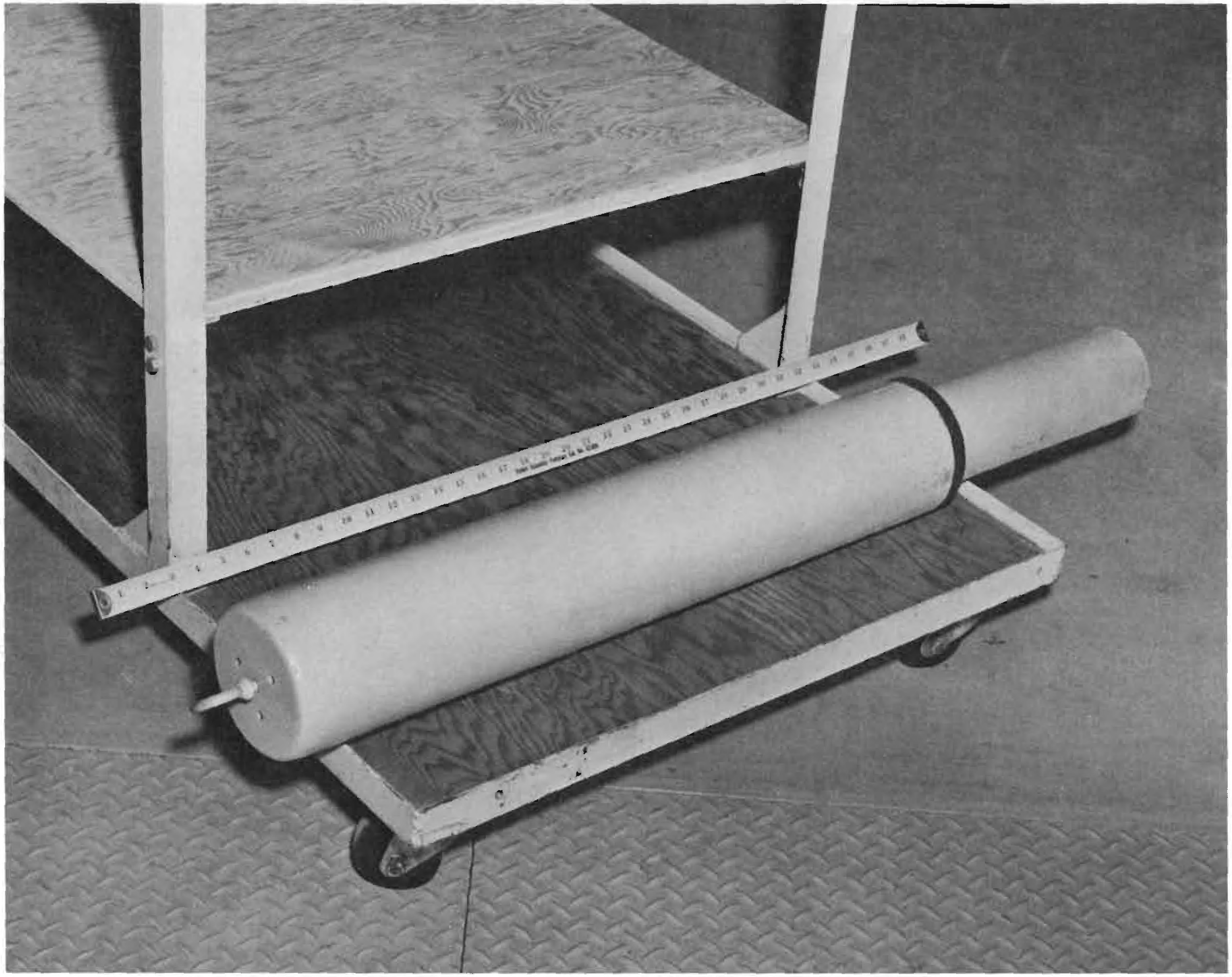

Fig. 8. Shielding Plug for Vertical Beam Hole

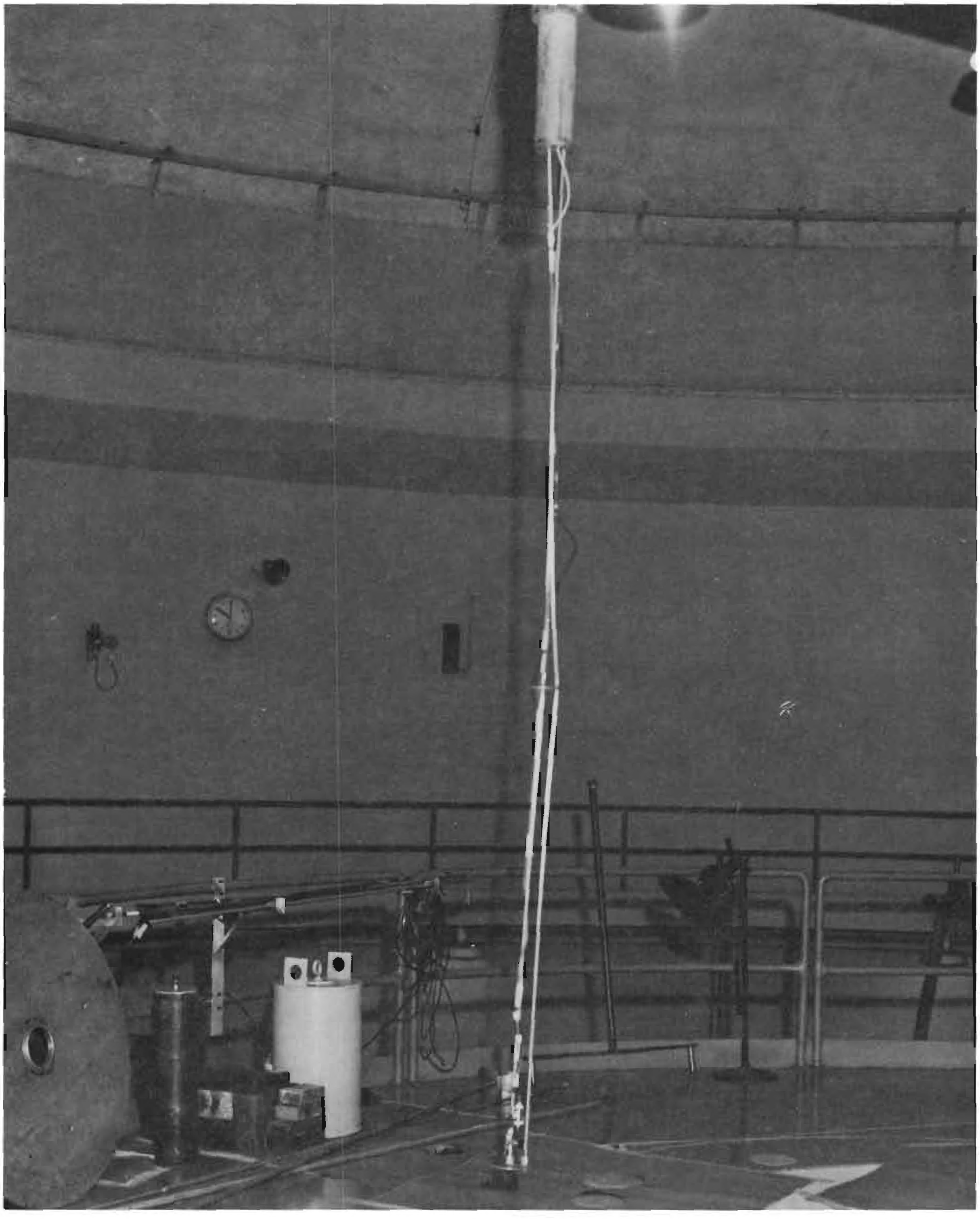

Fig. 9. Counter Assembly for Insertion into Vertical Beam Hole

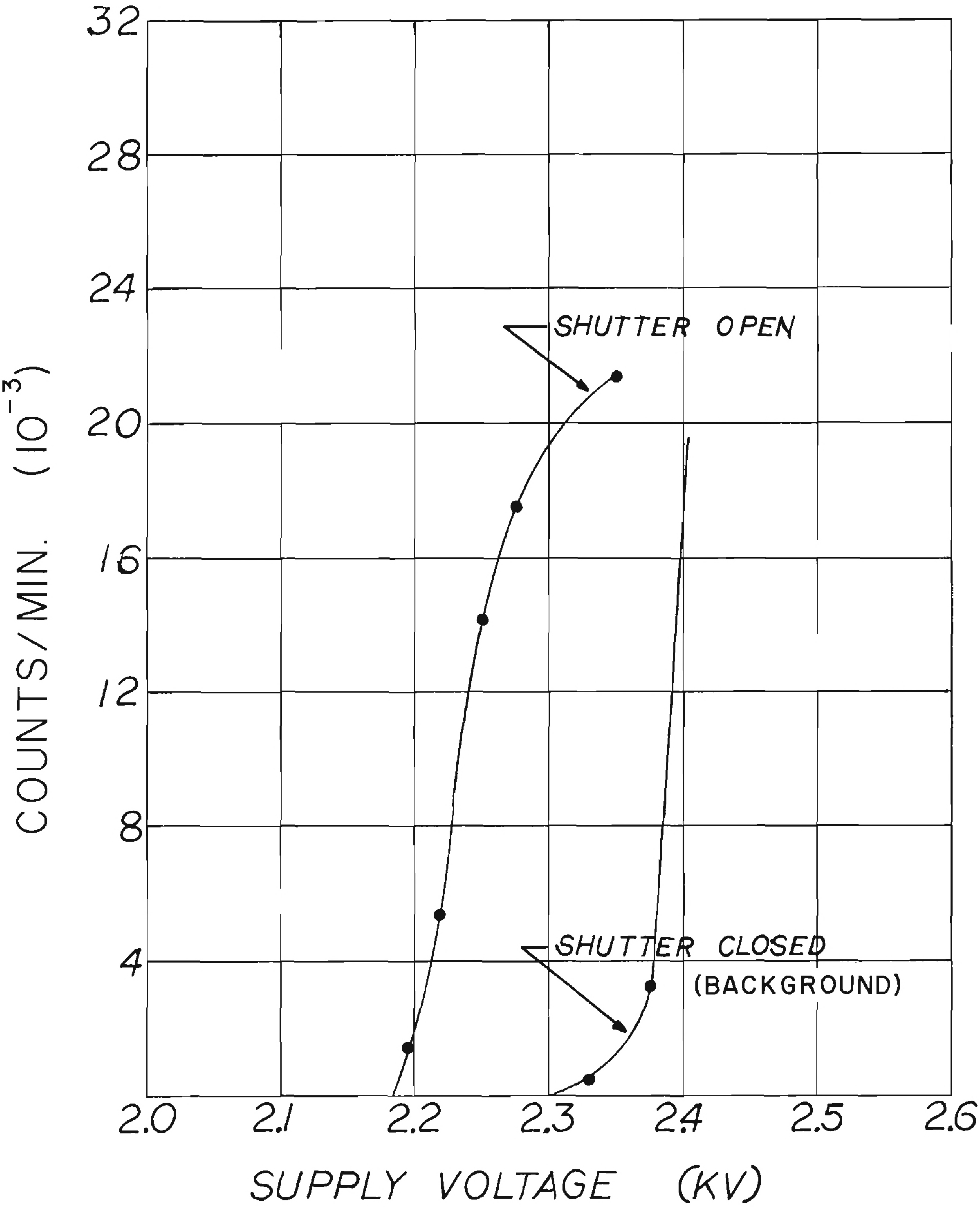

Fig. 10. Typical Counter Characteristic

reasonable range of voltages. The steep "background" curve arises from the dielectric breakdown condition which is triggered once a critical voltage is passed.

Since the current drawn under spark conditions is potentially rather high, it is important to operate the detector with a fairly high limiting resistor in series, which will effectively lower the operating voltage below the threshold. As a very large resistor would introduce a long time-constant and there is a danger of secondary electron avalanche formation in the discharge region, it becomes imperative to terminate the spark discharge as quickly as possible. While it was found helpful to use gases with a quenching impurity, such as helium with 0.95% isobutane, their quenching action did not appear to be fast enough to return the detector to its initial sensitive condition, in a time acceptable for fast count rates in high neutron fluxes. For this reason, it was decided to use external quenching by means of a circuit capable of cutting off the detector voltage a few microseconds after initiation of the spark.

This circuit underwent many modifications and is shown in its final form in Fig. 11. This circuit is a triggered flip-flop, capable of switching the high voltage to the detector on and off, in one and five to ten microseconds, respectively. It was found that, when the high voltage was restored too quickly, i.e. within 2-5 microseconds, afterpulses were observed due to insufficient removal of residual ions in the spark gap. This mode of operation was found preferable to the reverse operation of turning on the voltage for predetermined intervals, as is customary for spark chambers.

A notable feature of spark counters is, of course, their large signal

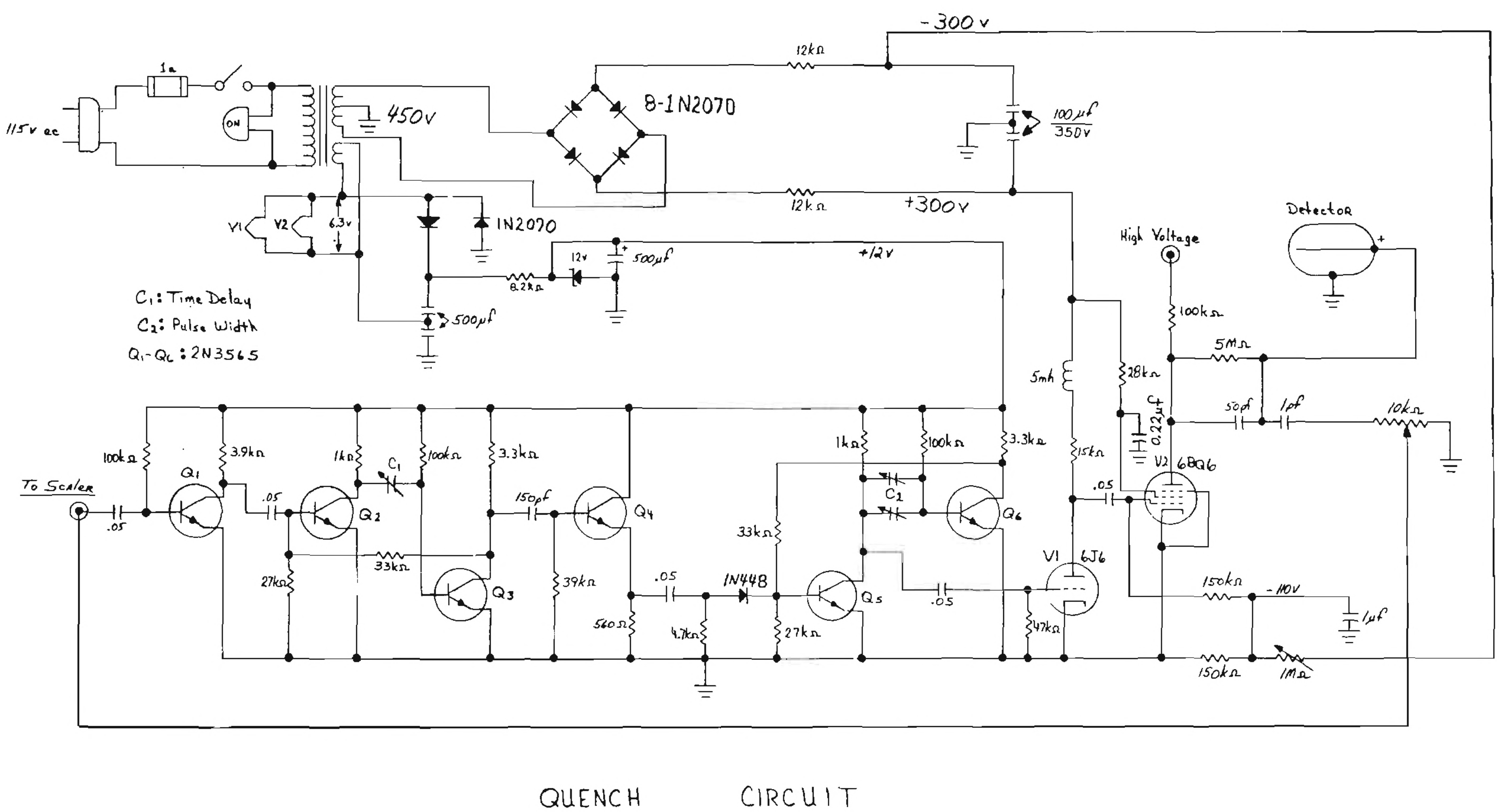

Fig. 11. Quench Circuit

amplitude, commonly of the order of 30-40 volts. Whereas other detectors require considerable signal amplification, with all the attendant noise problems, the spark counter signal must be reduced in amplitude in a voltage divider, so that it can be counted easily in a conventional scaler and to avoid undesirable feedback along the high voltage lines. The divider is also shown in Fig. 11.

Converter Material

The earlier neutron detectors had introduced the boron converter by coating Lucite chips or disks with a thin layer of boric acid, H_3BO_3. Since this was unsuitable for high-temperature operation, it was decided to use a more stable, machineable material in disk form. The most convenient material of that type is boron nitride, BN, made by Union Carbide as type HBR boron nitride in easily machineable form and available both in rod or washer form. Earlier experiments used disks machined from rod, that were relatively thick. Later tests with the small counter have used $\frac{3}{4}$" washers, 0.0625 inch thick, which are readily available as a standard product. The manufacturer quotes measurements on mechanical properties at 1830° and 2750°F so that this material may be expected to hold up satisfactorily over the temperature range required.

Some inquiries have been made concerning the availability of boron compounds enriched in boron-10. It appears that the yield and cost would be out of proportion to the benefits gained, particularly as high detector efficiency is not required at this time. The question of possible depletion of boron-10 in commercial boron compounds was considered, but no evidence was found for this in the material used.

A major concern was being felt concerning the self-heating of the BN washers by neutron absorption; in fact, insertion of the detector into the reactor was being delayed until this factor had been measured. For this purpose, two runs were made on BN disks mounted between two aluminum washers. They were placed into beam port H2 on the graphite stringer in two positions and their temperature was measured while the reactor was brought to full power in slow stages. The temperature was followed for the next 10 hours while the reactor shield approached equilibrium temperature.

The results of these measurements are shown in Fig. 12. It is seen that, even at 10^{12} n/cm^{2}sec, the boron nitride runs only about 14°F above the temperature of the surrounding graphite. In higher fluxes and at higher temperatures, the neutron absorption is not felt to be a serious source of additional heat, particularly if the detector is inserted so as to provide good heat transfer to and from its surroundings.

For very high neutron fluxes, it may prove preferable to return to thin boron coatings on a ceramic disk surface. Under those conditions, very little converter surface would be needed anyhow to avoid overloading the detector. A thin converter would tend to minimize flux depression.

Determination of Counter Characteristics

The parameters of primary importance with any radiation detector are the useful operating range and the attainable signal-to-background ratios. Operating characteristics have been measured and plotted for all the detector systems used, for different gas fillings, different gap spacings, and different sources.

Figure 12 shows a representative characteristic curve, this one ob-

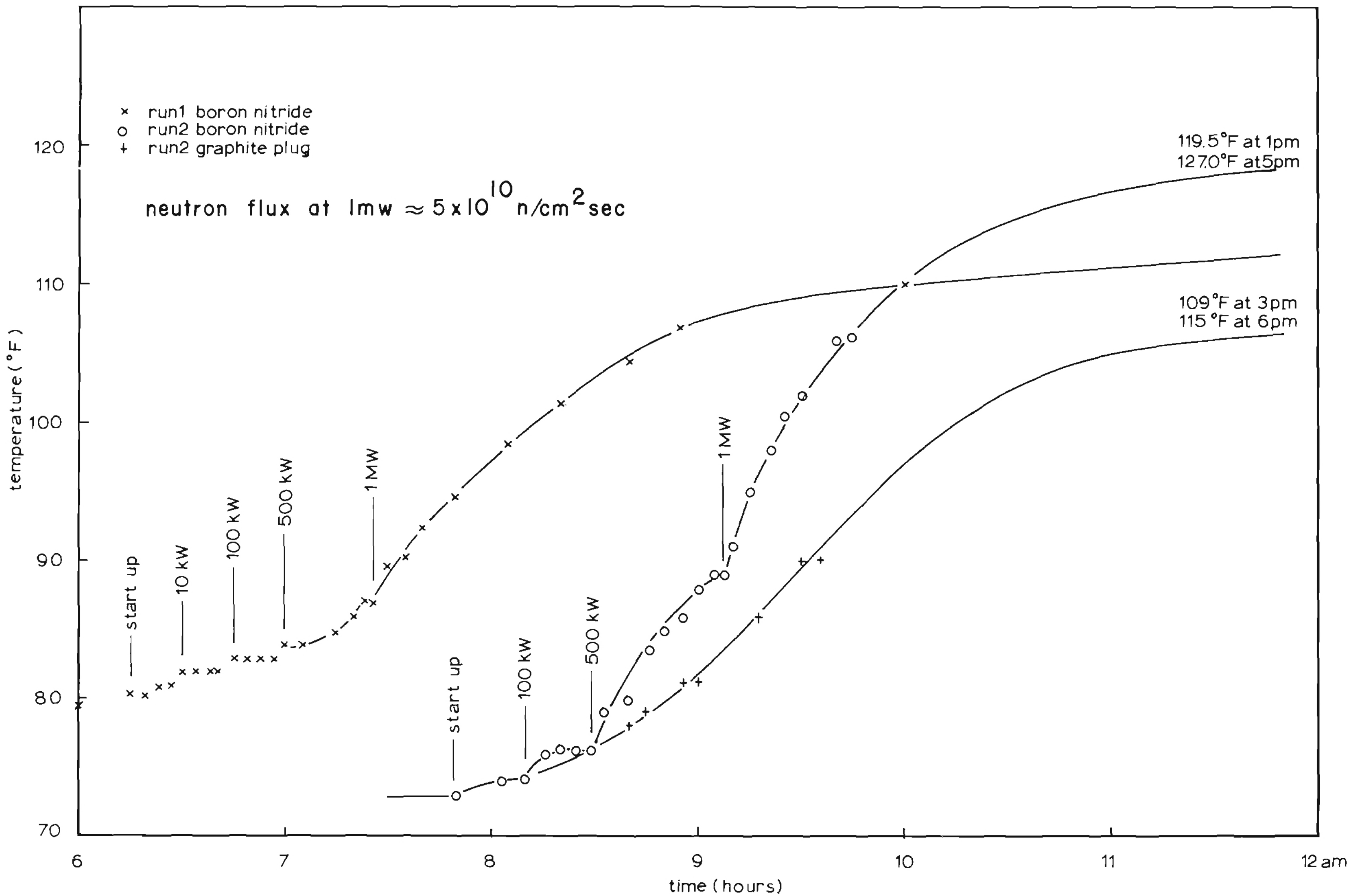

Fig. 12. Boron Nitride Heating Curves

tained at the reactor face for the stainless steel detector with pure argon gas filling. It shows all the features typical of the spark counter operation.

To start with, there is no "plateau" in the sense used with Geiger tubes. The count rate increases with voltage, starting at a threshold of operations in a slightly nonlinear fashion. This increase is presumably related to the greater extent of the corona region as the voltage is increased and hence the greater sensitive volume from which ions can trigger spark discharges. The background count is seen to be practically zero until a breakdown voltage is reached above which uncontrolled discharge may occur, limited only by the characteristics of the quenching circuit. The area between the two curves represents the useful operating region. An operating voltage about 30-50 volts above the threshold constitutes the best compromise for high signal-to-background ratio and adequate efficiency. The steepness of the operating curve requires reasonable stability of the power supply. It should be noted that the voltage plotted represents the supply voltage under quiescent conditions; the actual voltage across the detector at high count rates may be considerably lower. This may account for some of the nonlinearity of the operating curve.

Figure 13 presents comparable characteristics for neutron detection for two different gap spacings in the large detector with helium-isobutane filling. The curves are similar, but as expected the operating voltage is higher for the wider spacing. Similar curves have been obtained for argon and helium gas fillings, but the results tended to be more erratic. After adjusting some of the parameters in the quenching circuit, the argon data obtained became much more consistent.

Comparative operating curves were also obtained for different numbers

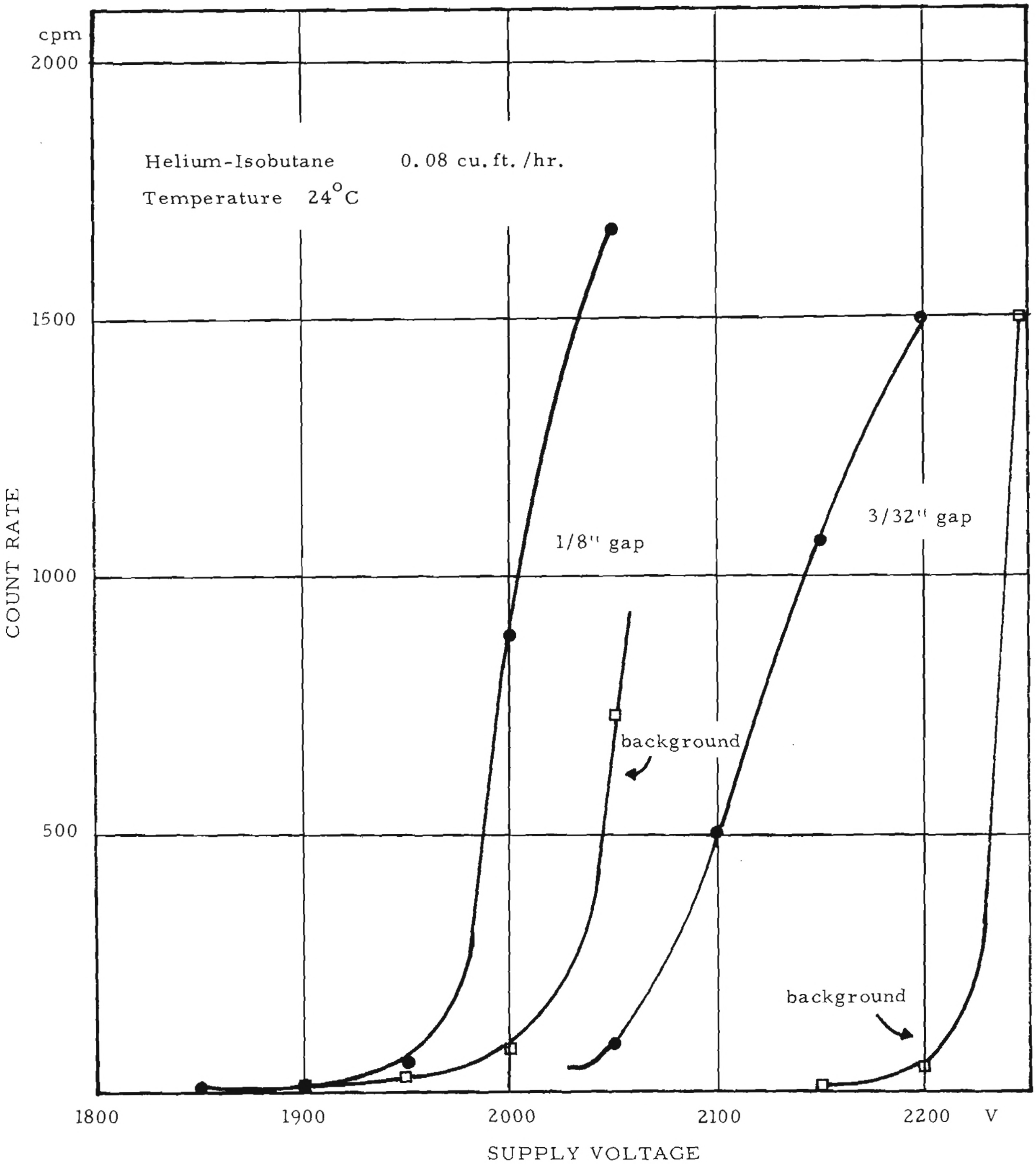

Fig. 13. Effect of Gap Width on Operating Characteristics

of electrodes. Figure 14 shows the results for two-gap, 3 boron washer, and four-gap, 5 boron washer arrangements, which show a much longer operating region for the longer assembly. Using aluminum and gold foils for flux calibrations, a rough estimate was made of the efficiencies of the two assemblies, making allowance for the difference in effective size. At the midpoint of the characteristic curve, the count rate was 4000 c/min in a flux of 8×10^7 n/cm^{2}sec for the 1 inch "short" steel detector, with two gaps and argon filling, corresponding to a sensitivity of 6.7×10^{-8} counts per incident neutron. For the small aluminum detector, with four BN disks and He + isobutane filling, the count rate was 1300 c/min in a flux of 3.28×10^6 n/cm^{2}sec, corresponding to a sensitivity of 5.8×10^{-7} counts per incident neutron. This is of the right order for permitting reasonable count rates in higher fluxes considering the time constants of the circuit used.

Filling Gases

The ionization characteristics and spark development depend crucially on the nature of the filling gas, its pressure and purity. Gases used have been Matheson high purity helium, argon, helium + 0.95% isobutane, and argon + 1% nitrogen mixtures. Most of the early measurements were done with helium-isobutane mixture in slow flow, since this operation tended to lead to the most consistent results. Maintenance of constant flow rate was important, as the flow was controlled largely by deliberate leakage paths from the detector, so that different flow rates implied different gas pressures. Figure 15 shows an extreme case of this situation for argon.

Although the presence of an internal quencher like isobutane helped to stabilize counter operation, the presence of an organic impurity was considered undesirable for in-core neutron monitoring and all later tests were done with Ar, He, or Ar+N_2. Figure 16 shows the very wide character-

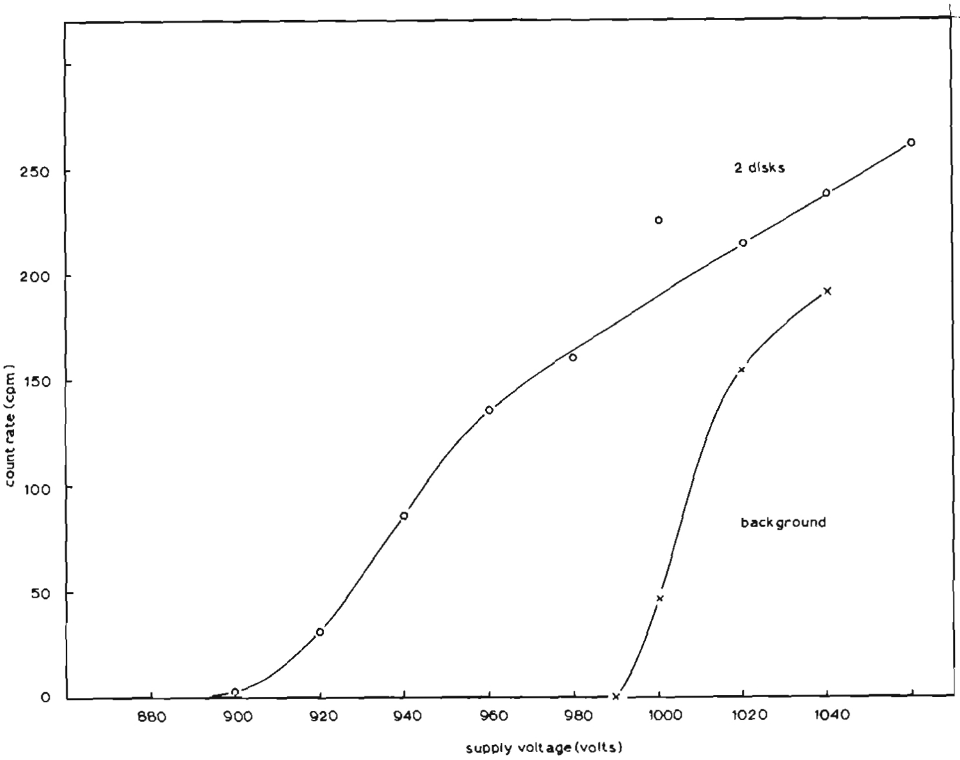

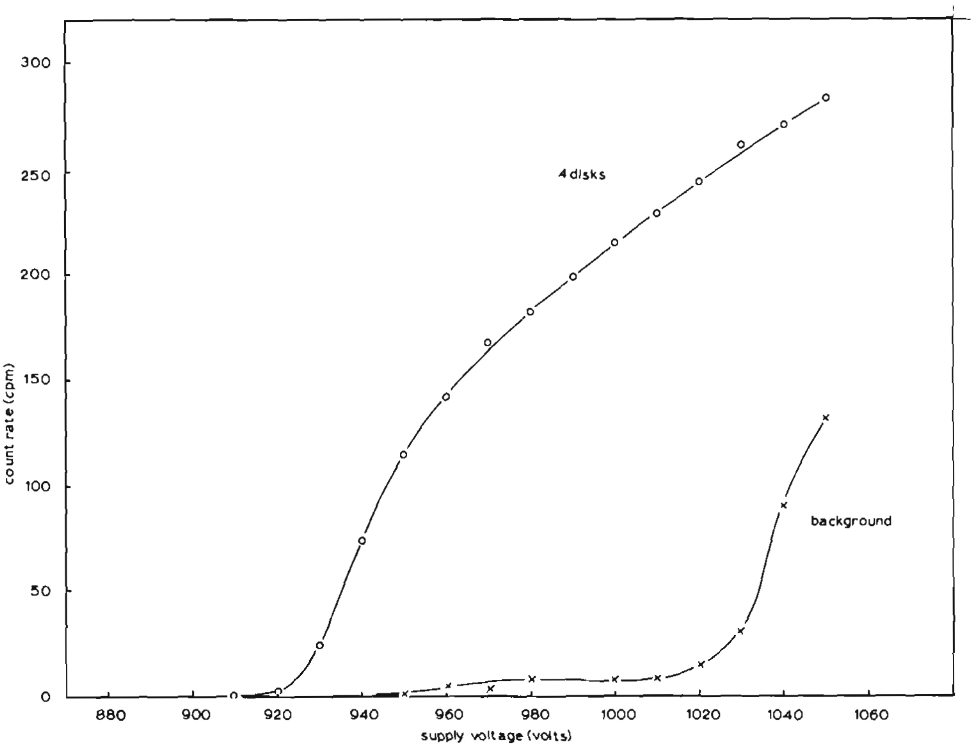

Fig. 14. Variation in Gap Number -- Effect on Operating Characteristics

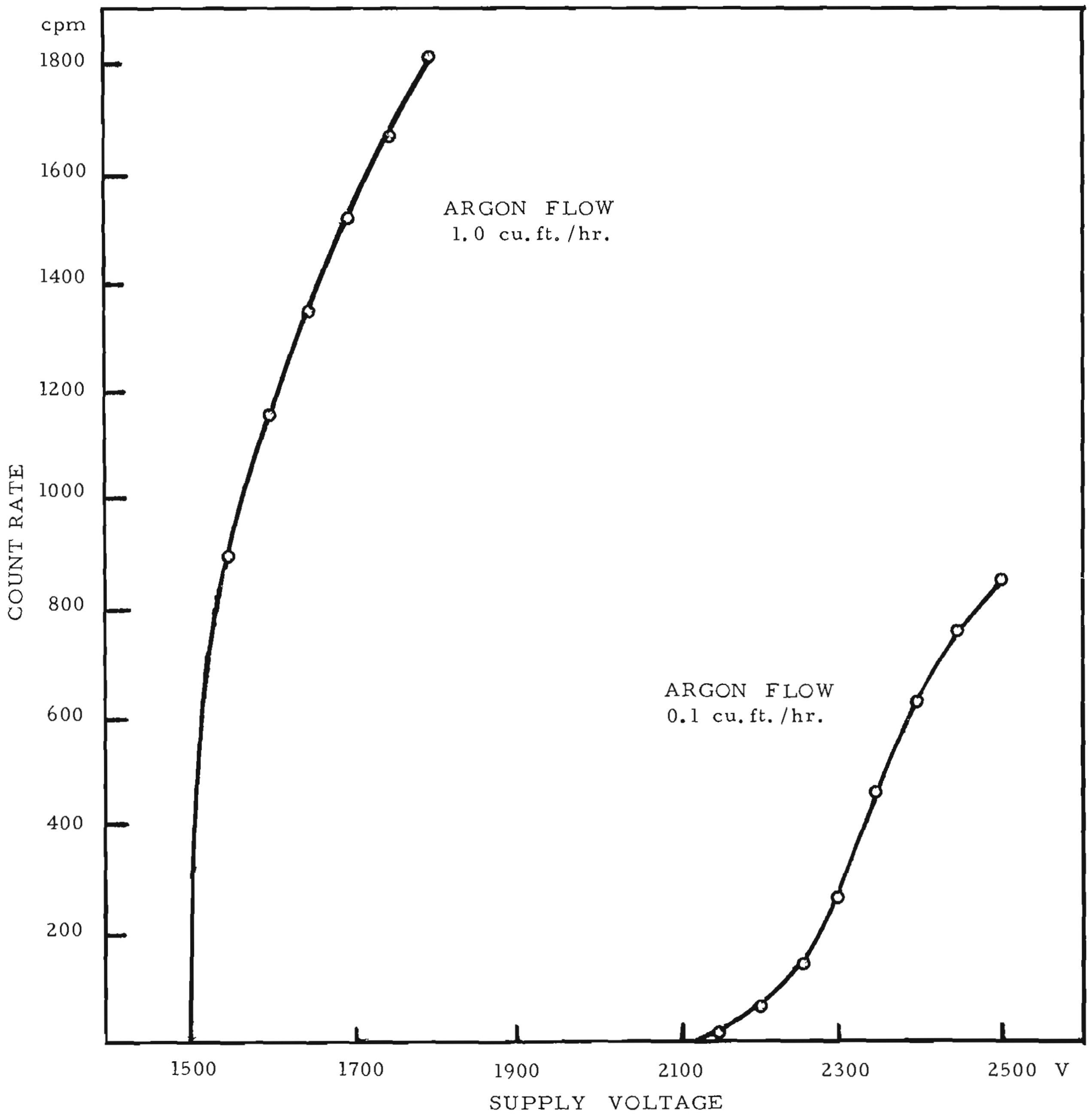

Fig. 15. Effect of Flow Rate on Counter Characteristics

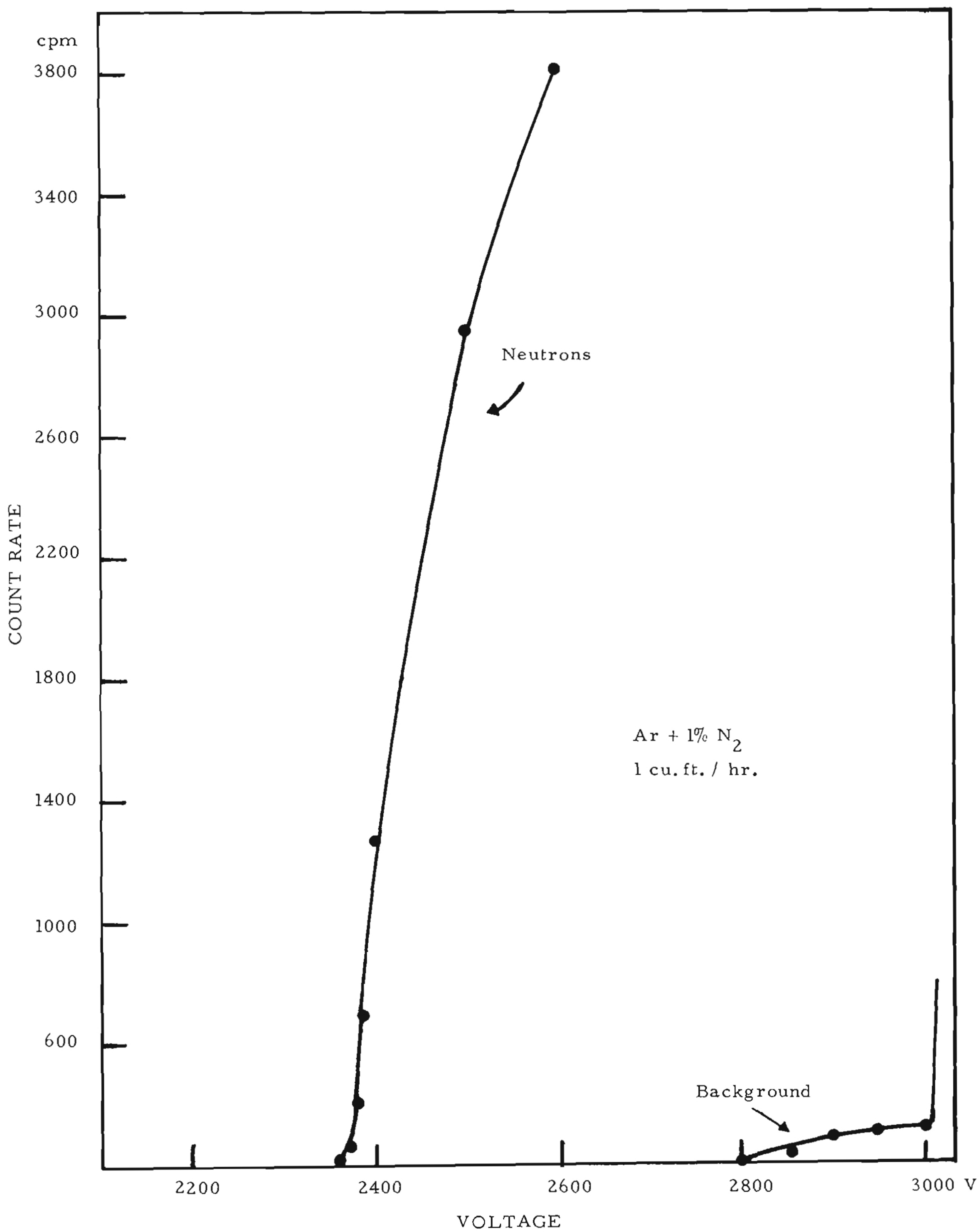

Fig. 16. Operating Characteristics for Stainless Steel Detector, Ar-N_2 Filling

istics obtained for the stainless steel detector with the argon-nitrogen mixture.

For high-level neutron runs, one of the stainless steel detectors was sealed off by means of a needle valve. This arrangement is shown in Fig. 17. After careful baking out, this detector could be operated at gas pressures varying from 10 to 760 Torr. Leakage rates were found to be small compared with the time required for the various tests. Most of the tests at reduced pressure were done with argon and argon + nitrogen mixture and will be discussed below.

Operating Range

Of primary concern in operating the detector is its linearity, i.e. the proportionality between counts recorded and incident neutron flux. Figure 18 presents the results for the stainless steel detector, with pure argon, operated at a detector voltage of 2300 V as determined by a digital voltmeter connected across the detector. It is seen that up to a flux of 10^8 n/cm^{2}sec, as available in the Medical Facility, the detector was perfectly linear.

The sensitivity to gamma-ray background radiation was also checked at the face of the reactor, by comparing the bare detector with count rates obtained while it was wrapped in cadmium sheet. It was found that, in the presence of a gamma field of 50 R/hr, comparable to the neutron field, the gamma-ray contribution was negligible while the neutron count rate was about 5300 cpm. The neutron flux was about 6×10^8 n/cm^{2}sec.

To measure the response of the counter at higher flux levels, it was mounted on a frame as shown in Fig. 9 and lowered into a vertical

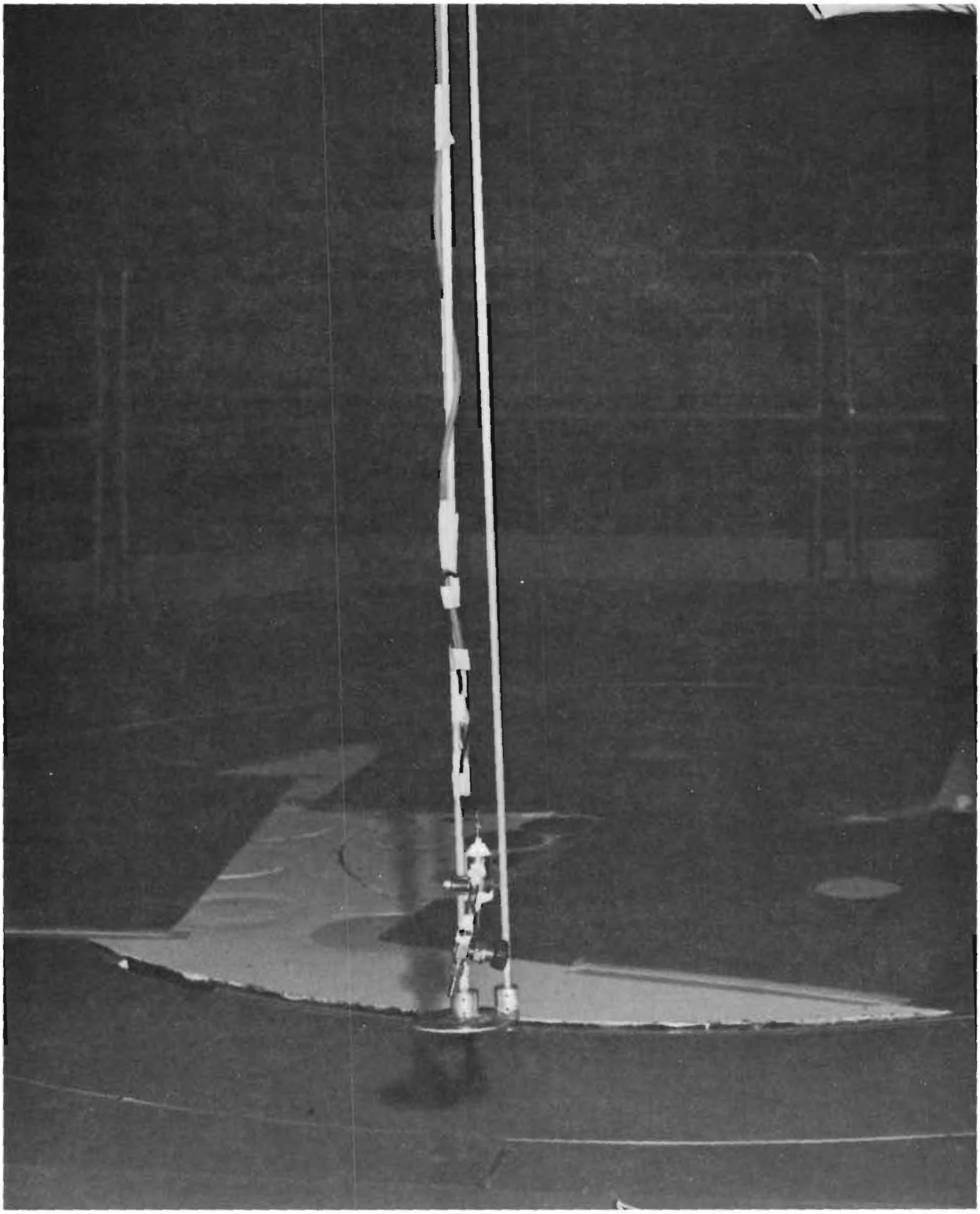

Fig. 17. Close-up View of Stainless Steel Detector with Needle Valve

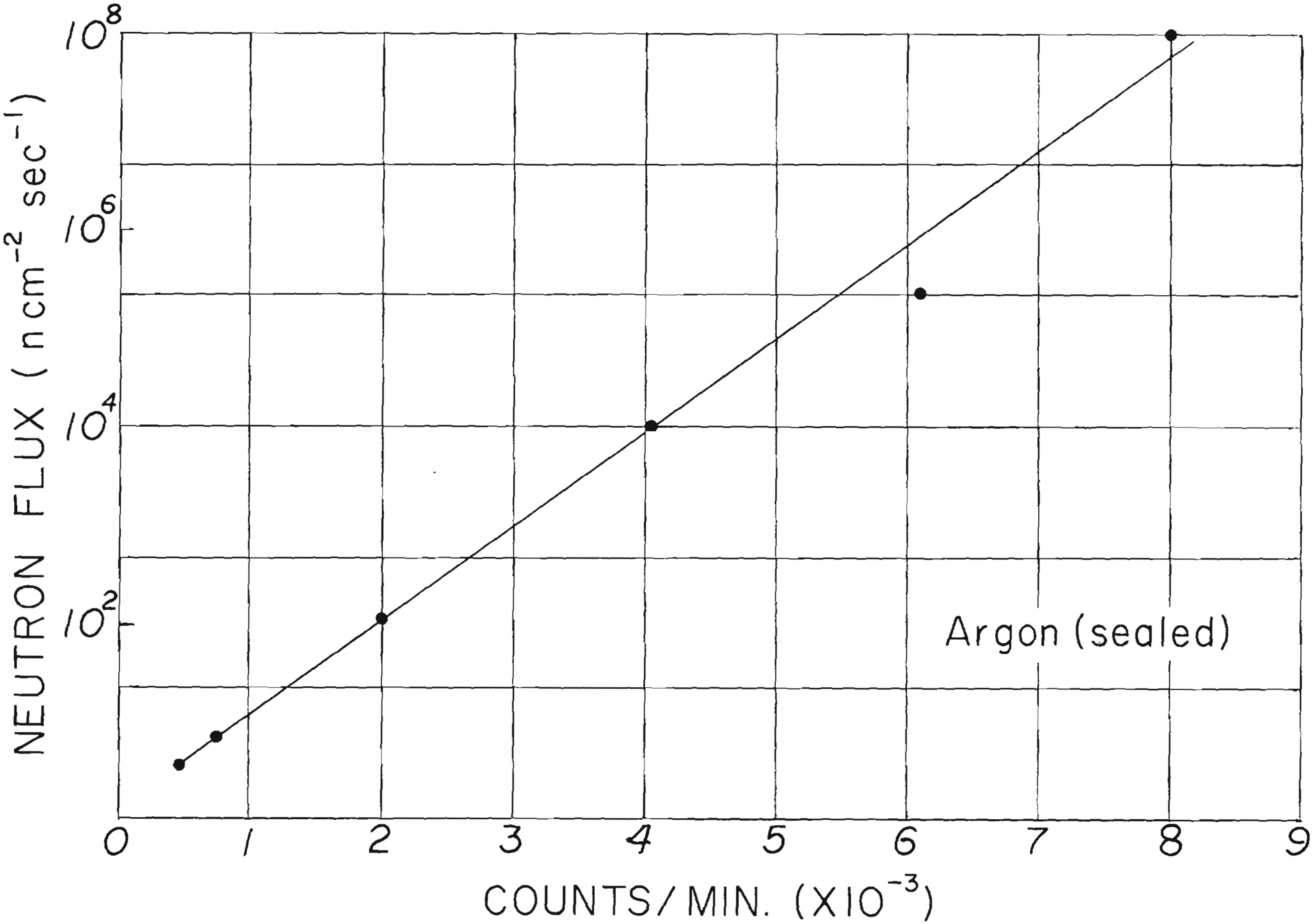

Fig. 18. Linearity Plot -- Relation of Count Rate to Neutron Flux

beam hole to a position close to the centerline of the reactor core. A rhodium-rhodium/palladium resistive flux monitor was fixed alongside to check neutron flux levels. Since the rhodium monitor is essentially a neutron heating device, it was found that its response to changes in neutron flux was much slower than that of the spark counter. For the tests, the reactor power was raised in steps from start up, with each step being long enough to obtain adequate counts and for the flux monitor to attain equilibrium.

It was found that response linearity was maintained up to a neutron flux of about 10^{10} $n/cm^2 sec$. Above that level, the corona current increased steadily with reactor power, presumably due to growing ionization of the counter gas by primary or secondary gamma radiation. This is shown by the data in Table 1, which present the experimental results of such a run using argon at 760 Torr. As the corona current increased, it became necessary to raise the supply voltage to keep the detector voltage constant. However, even so spark formation was progressively reduced as the additionál, neutron-induced, ions became less and less significant compared with the steady current flow.

To reduce the rate of gamma-ray ionization, runs were conducted with air, argon, and argon+nitrogen at reduced pressure. However, the results were essentially similar to those obtained at atmospheric pressures. Figure 19 shows the variation in supply voltage needed to keep the detector voltage constant at different reactor power levels. Figure 20 illustrates the same effect in a different way by showing the supply voltage required to maintain a given count rate at different reactor powers. Both of these plots were obtained with argon at 100 Torr. Results with air were more er-

Table 1

Results of High Level Spark Counter Run No. 1

Argon at 760 Torr

Reactor Power (kW)	Neutron Flux (Rh monitor)	Gamma-ray Dose (R/hr)	Supply Voltage (kV)	Detector Voltage (kV)	Count Rate (cpm)
0.05	---		2.240		0.2
0.5	5×10^{7}		2.240		2
1	10^{8}		2.240	2.09	6
5	5×10^{8}	1.8×10^{3}	2.240	2.09	25
20	2×10^{9}	7×10^{3}	2.240	2.05	68
			2.260	2.08	78
60	6×10^{9}	2×10^{4}	2.260	1.99	21
			2.360	2.07	123
150	1.5×10^{10}	5×10^{4}	2.360	1.94	2
			2.600	2.06	(35?)
			2.660	2.08	65
300	3×10^{10}	10^{5}	2.660	1.97	--
			2.930	2.08	15
600	6×10^{10}	2×10^{5}	2.930	1.92	--
			3.430	2.08	1

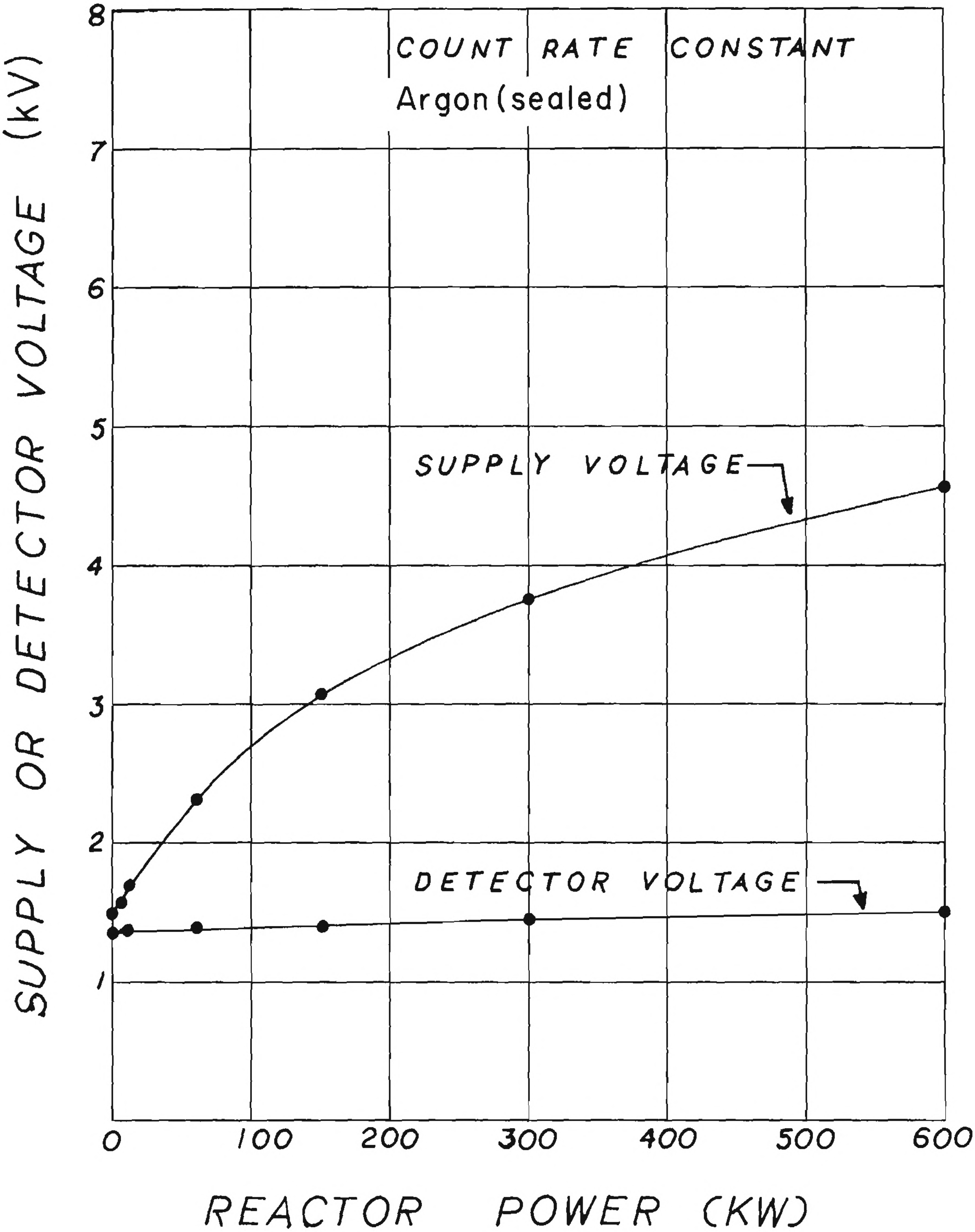

Fig. 19. Variation of Supply Voltage at High Flux Levels

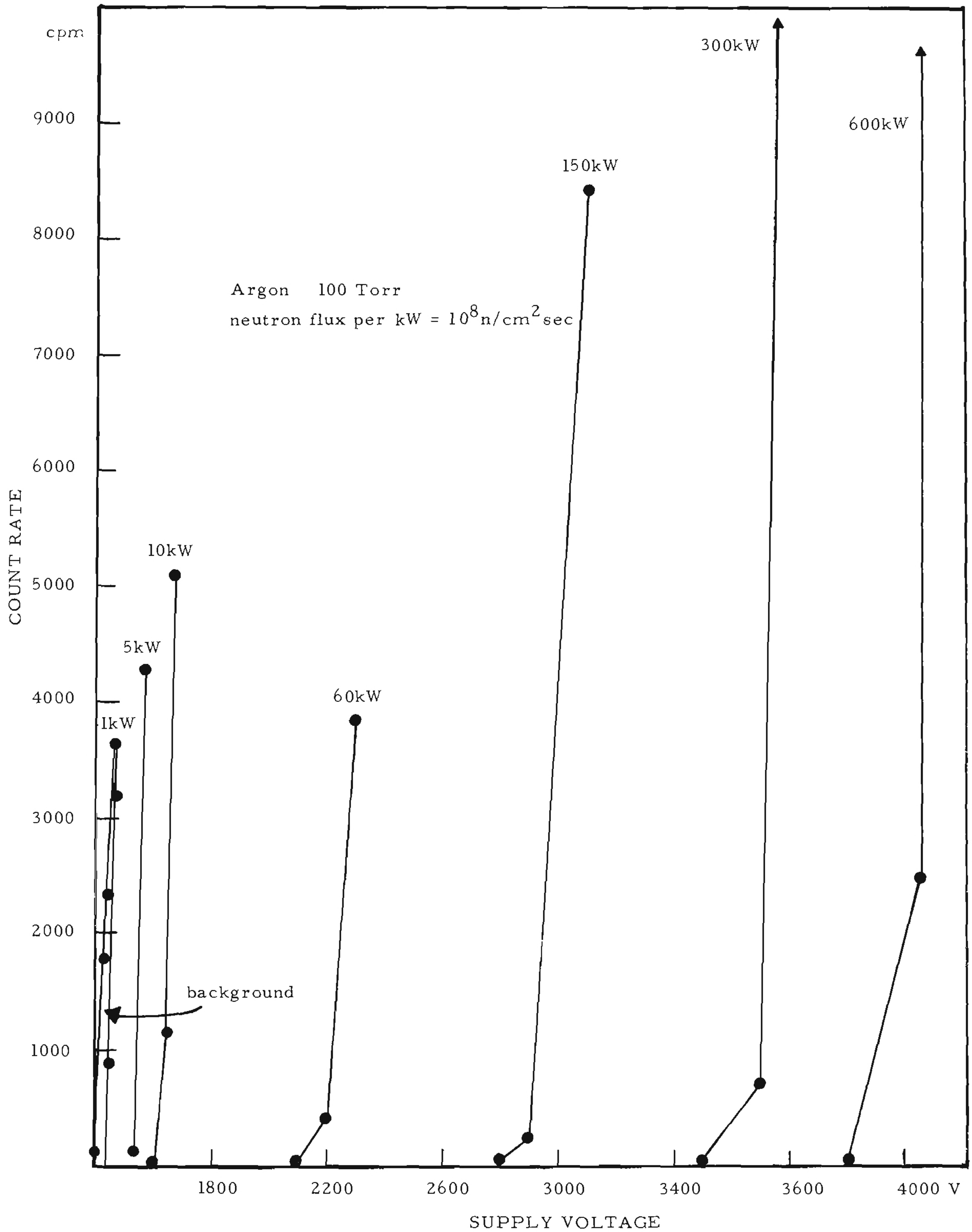

Fig. 20. Shift in Supply Voltage to Maintain Constant Counts

ratic.

These effects are sufficiently serious to make it questionable if any gas-filled spark counter can be expected to operate reliably at flux levels above 10^{10} $n/cm^2 sec$. In fact, the steady current could serve as an indication of ambient flux. No separate measurements could be done in the reactor without the corresponding gamma-ray field, so that it is difficult to assign the observed steady ionization current to either the gamma-ray background or to neutron capture. Attempts could be made to check the high-level gamma-ray sensitivity of the spark counters by exposure to the 12,000 curie cesium-137 source, available at Georgia Tech.

High Temperature Operation

One of the main objectives of this project was the development of a counter capable of operating at high temperatures. Accordingly, at each stage of development, parallel tests were conducted to observe high temperature performance. Figure 21 shows the Lindberg muffle furnace set up at the reactor face with a detector mounted in it, and Fig. 22 shows a simple test using heating tape wrapped around the detector. (The large barrel on the right is the beam catcher).

Two effects were observed as the temperature was raised; one was a steady downward trend in operating voltage, the other was a narrowing of the operating region. This effect is illustrated in Fig. 23 a and b, which show the operating characteristics over a range of temperatures for two different detectors. The counter sensitivity did not change significantly over the temperature range, as is seen from the constant "height" of the counter characteristics.

The aluminum detector was operated up to 680°F, the stainless steel one up to 1076°F. Above about 1080°F it was found that the leakage across the ceramic end seals made normal operation of the stainless steel detector practically impossible. Most of the shift in supply voltage shown in Fig. 23 is ascribed to the increase in leakage current across the ceramic seal. Figure 24 shows the variation in optimum supply voltage for the stainless steel detector as a function of temperature. Some leakage takes place at low temperatures, but the break in the curve occurs when leakage accounts for most of the drain of the power supply.

A variety of porcelain insulators and high temperature oxides has been leak tested over the desired temperature range. Figure 25 shows a typical

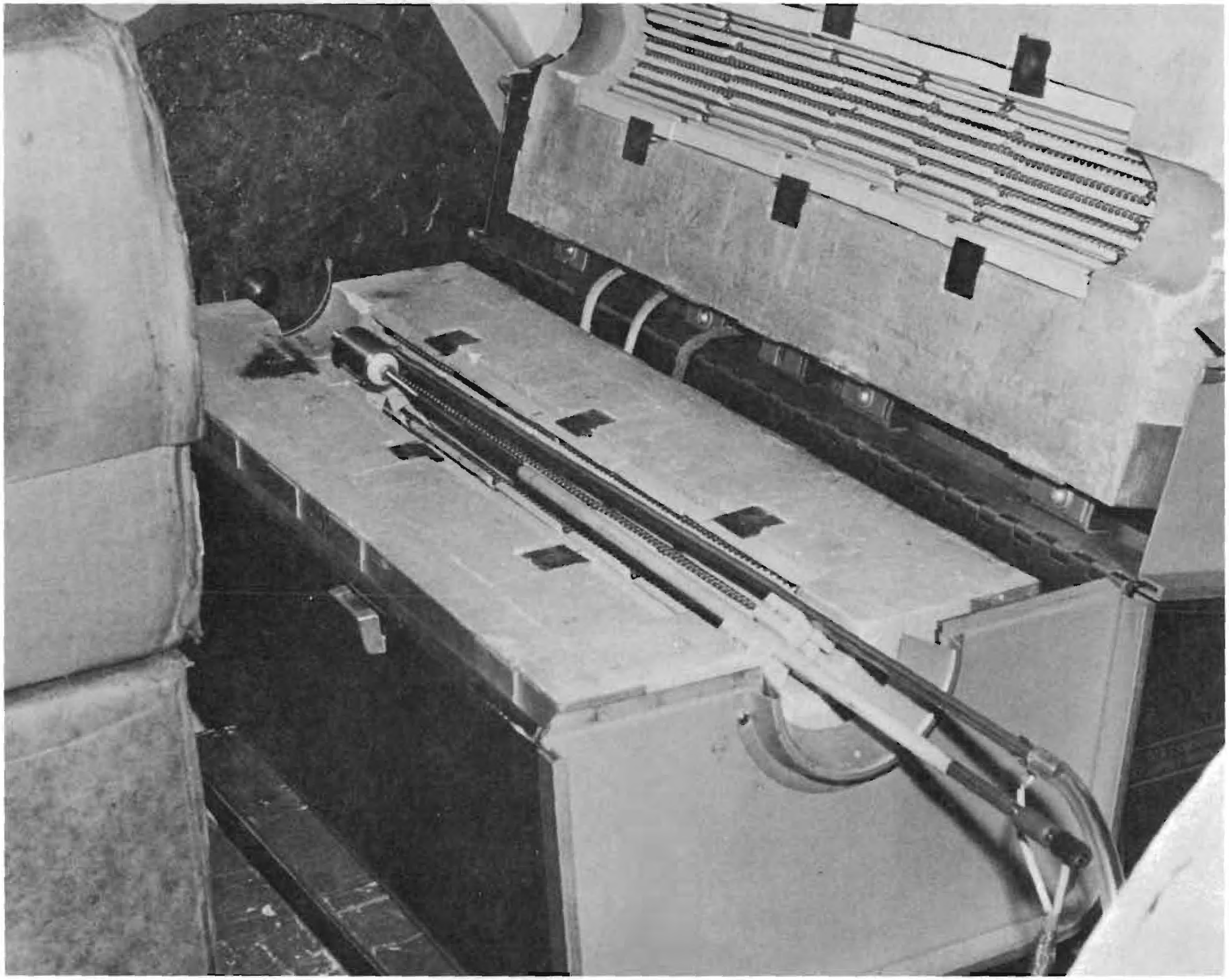

Fig. 21. Muffle Furnace Set Up at Reactor Beam Hole

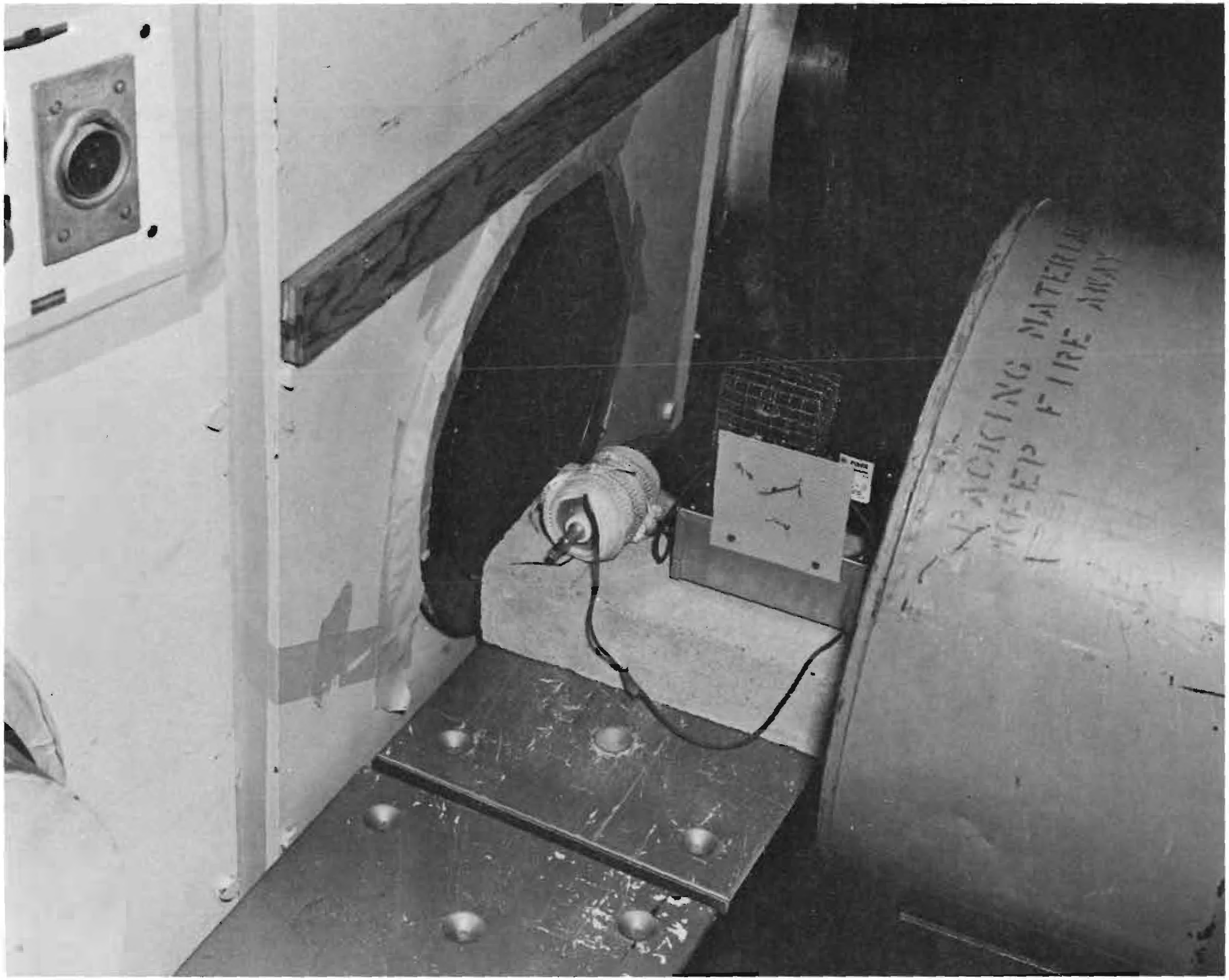

Fig. 22. View of Experimental Assembly at Beam Port

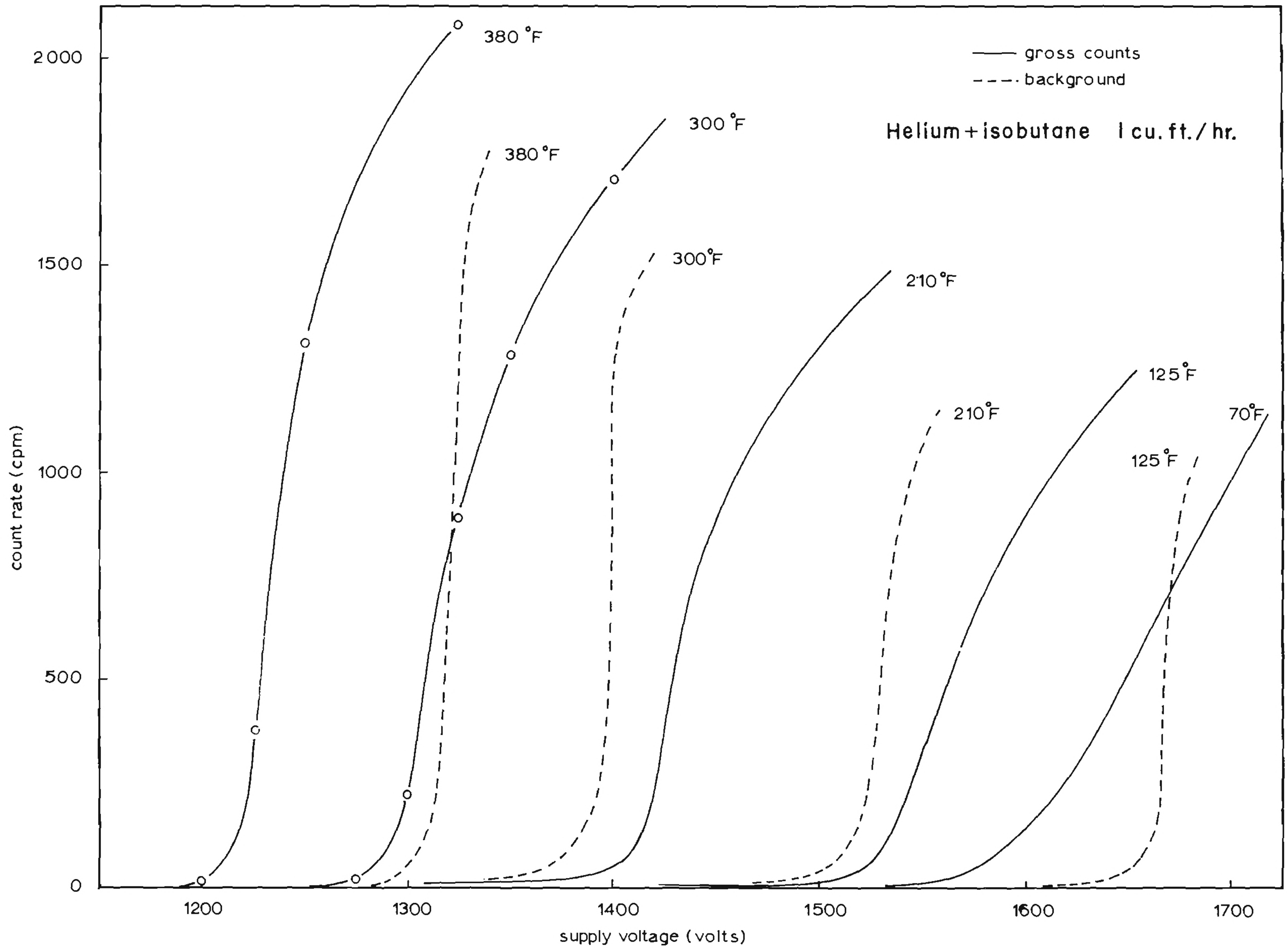

Fig. 23a. Temperature Characteristics of Spark Counter (large detector)

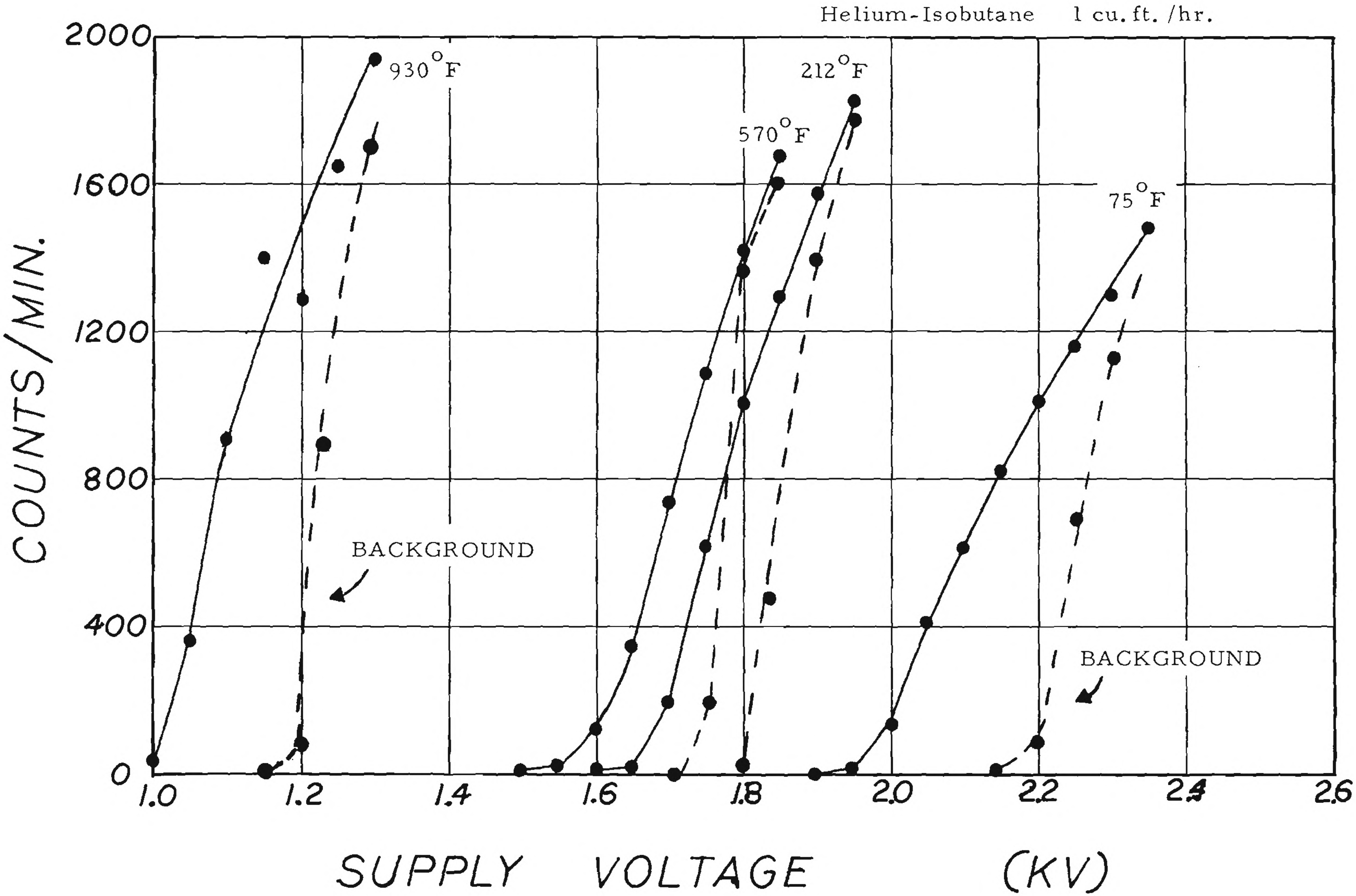

Fig. 23b. Temperature Characteristics of Spark Counter (small detector)

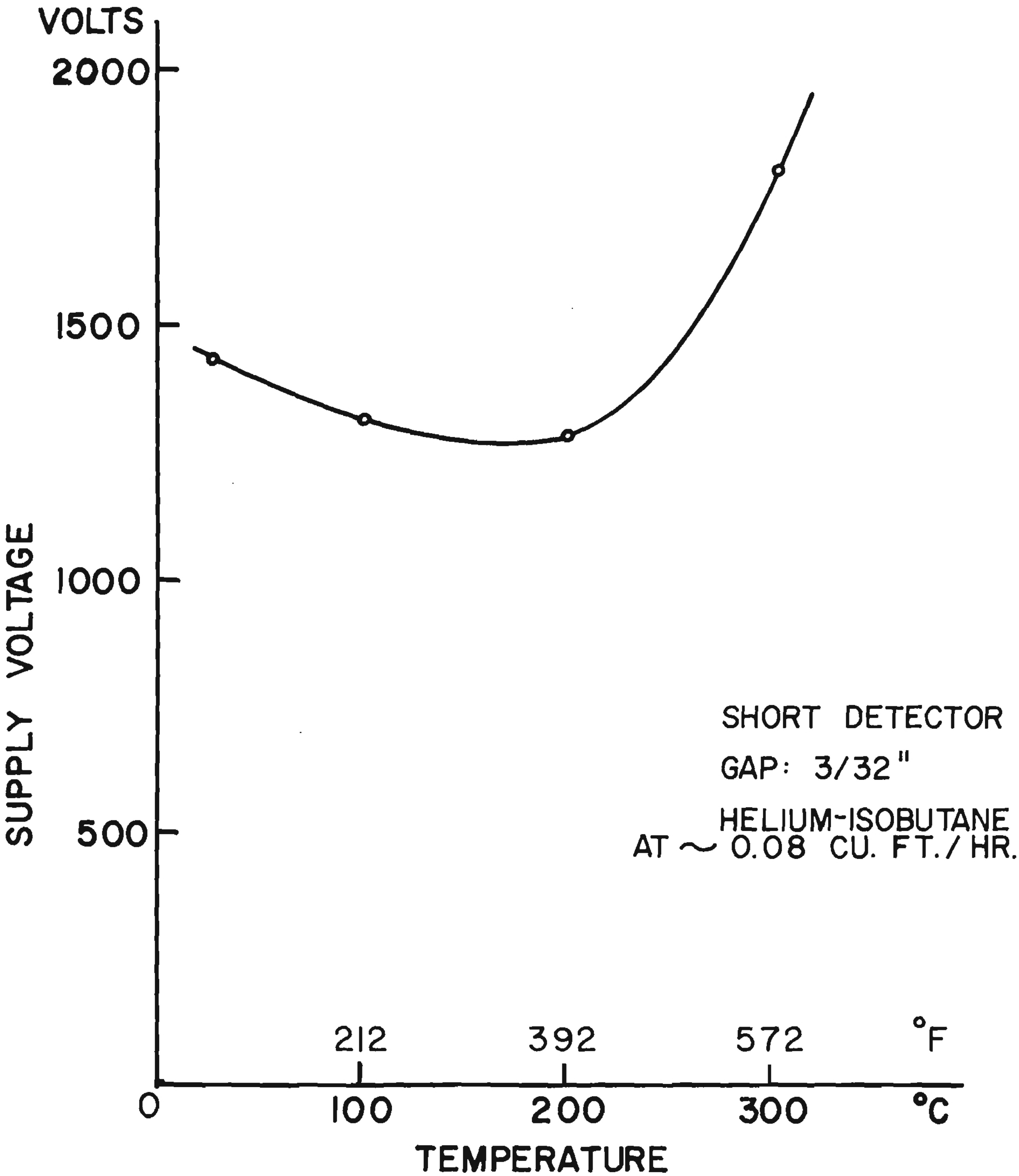

Fig. 24. Variation in Optimum Supply Voltage with Temperature

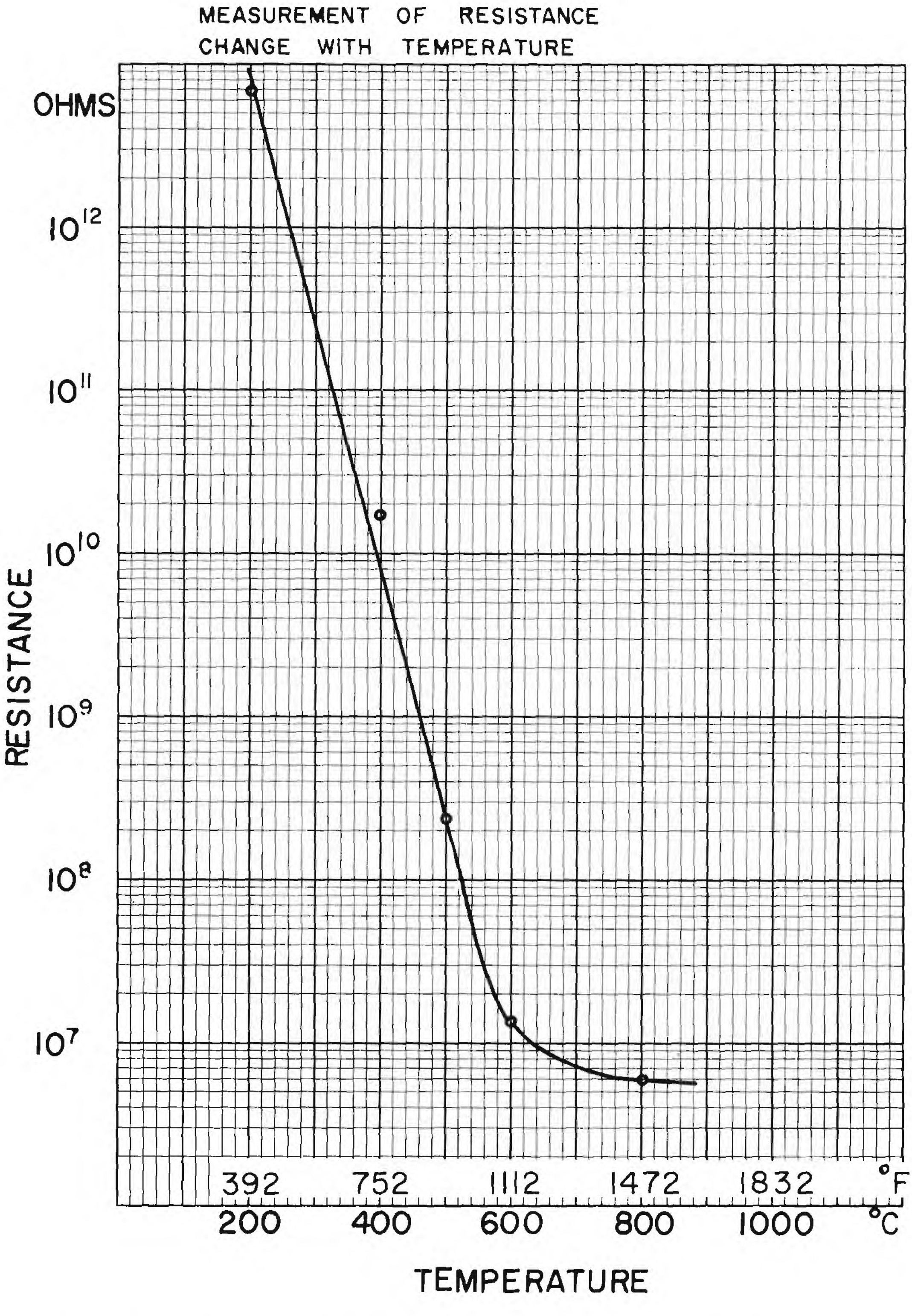

Fig. 25. Resistance-Temperature Plot for Porcelain Insulator

curve showing the decrease in resistance with temperature of a number of representative glazed porcelain insulators (U. S. Stoneware, Al Si Mag, etc.). Other materials, like various Sauereisen cements, were found to lose their insulating properties irreversibly on heating and were unsuitable for this application.

Conclusions

It has been shown that compact, cylindrical, gas filled spark counters operating as neutron detectors can be constructed and operated reliably. These counters are simple in construction, rugged, and provide a large signal pulse so that no amplification is required. External quenching has been found advantageous to avoid after-pulsing. The efficiency of the detector depends on size and on the number of converters and spark gaps employed.

The spark counters have been operated at temperatures up to 1076°F, the limit being set mainly by the leakage characteristics of the ceramic seals. As better seals become available, it should be possible to extend the temperature range to much higher values.

In terms of counter response, linear neutron detection has been obtained in neutron fluxes up to 6×10^9 n/cm^{2}sec, in the presence of gamma-ray fields of up to about 10^4 R/hr. Above that level, gas ionization becomes continuous and inhibits spark formation. The prime advantages of these detectors in the usable range of neutron flux levels are the high signal-to-background ratio and the high gamma ray rejection rate, with an almost negligible gamma-ray sensitivity in gamma fields below 1000 R/hr.

Project Personnel

The following staff members and student assistants have worked on this project for various periods.

Dr. Geoffrey G. Eichholz (Project Director)

Dr. Don S. Harmer

Mr. Robert J. Lord

Mr. James D. Phillips

Mr. Gary A. Griffith

Mr. A. Frank Stringfellow

Mr. Edward T. Chow

Mr. Larry A. Phillips

In addition, substantial assistance was rendered by Mr. Robert E. Meek and the Electronics Group of the F. H. Neely Nuclear Research Center, Mr. R. S. Kirkland and the operators of the Georgia Tech Research Reactor, and by the main machine shop of the Engineering Experiment Station.

References

1. G. G. Eichholz, "The Rosenblum Spark Counter," Nucleonics 10, No. 10, 46-49 (1952).
2. G. G. Eichholz and W. M. Templeton, "Corrugated Plate Spark Counters," Canad. J. Phys. 44, 229-235 (1966).
3. G. G. Eichholz and W. M. Templeton, "Neutron Detection by Corrugated Spark Counters," IEEE Trans. Nucl. Sci. NS-13, 725-728 (1966).
4. J. W. Hilborn, "Self-powered Neutron Detectors for Reactor Flux Monitoring," Nucleonics 22, No. 2, 69-74 (1964).
5. A. Goodings, "Developments in High Temperature Neutron Detectors," U. K. AEA Rept. AEEW-R 383 (1964).
6. W. H. Todt, "An In-core Radiation Detector for Monitoring Pulsed Reactor Excursions," Nuclear Appl. 5, 173-178 (1968).
7. R. C. Hawkings, "Neutron Flux Monitors and Thermocouples for In-core Reactor Measurements," AECL Report AECL-2033, Chalk River, Ont. (1964).
8. R. P. Shutt (ed.), Bubble and Spark Chambers, Academic Press, New York, 1967.
9. P. Rice-Evans, "Spark and Streamer Chambers," J. Sci. Instr. (Ser. 2) 2, 221-229 (1969).
10. J. Bounin, R. H. Miller, and M. J. Neumann, "Automatic Retrieval Spark Chambers," Methods in Comput. Phys. 5, 1-46 (1966).
11. G. G. Eichholz, "Spark Counter Neutron Detector for High Temperature Applications," Annual Summary Report, Contract No. AT-(40-1)-3563, July 1967.